Duncan, R.A., Tarduno, J.A., Davies, T.A., and Scholl, D.W. (Eds.)
Proceedings of the Ocean Drilling Program, Scientific Results Volume 197

1. Leg 197 Synthesis: Southward Motion and Geochemical Variability of the Hawaiian Hotspot[1]

Robert A. Duncan,[2] John A. Tarduno,[3] and David W. Scholl[4]

ABSTRACT

The bend in the Hawaiian-Emperor volcanic chain is an often-cited example of a change in plate motion with respect to a stationary hotspot. Growing evidence, however, suggests that the bend might instead record variable drift of the Hawaiian hotspot within a convecting mantle. Paleomagnetic and radiometric age data from samples recovered during Ocean Drilling Program (ODP) Leg 197 define an age-progressive paleolatitude history, indicating that the Emperor Seamounts volcanic trend was formed principally by rapid (4–5 cm/yr) southward motion of the Hawaiian hotspot during Late Cretaceous to early Tertiary time (81–47 Ma). Paleointensity data derived from Leg 197 suggest an inverse relationship between field strength and reversal frequency, consistent with an active lower mantle that controls the efficiency of the geodynamo. Petrochemical data and observations of volcanic products (lava flows and volcaniclastic sediments) from Detroit, Nintoku, and Koko Seamounts provide records of the evolution of these volcanic systems for comparison with recent activity in the Hawaiian Islands. We find that the Emperor Seamounts formed from similar mantle sources for melting (plume components and lithosphere) and in much the same stages of volcanic activity and time span as the Hawaiian volcanoes. Changes in major and trace element and Sr isotopic compositions of shield lavas along the lineament can be related to variations in thickness of the lithosphere overlying the hotspot that control the depth and extent of partial melting. Other geochemical tracers, such as He, Pb, and Hf isotopic compositions, indicate persistent contributions to melting from the plume throughout the volcanic chain.

[1]Duncan, R.A., Tarduno, J.A., and Scholl, D.W., 2006. Leg 197 synthesis: Southward motion and geochemical variability of the Hawaiian hotspot. *In* Duncan, R.A., Tarduno, J.A., Davies, T.A., and Scholl, D.W. (Eds.), *Proc. ODP, Sci. Results,* 197, 1–39 (Online). Available from World Wide Web: <http://www-odp.tamu.edu/publications/197_SR/VOLUME/SYNTH/SYNTH.PDF>. (Cited YYYY-MM-DD)
[2]College of Oceanic and Atmospheric Sciences, Oregon State University, 104 Ocean Administration Building, Corvallis OR 97331-5503, USA. **rduncan@coas.oregonstate.edu**
[3]Department of Earth and Environmental Sciences, University of Rochester, 227 Hutchison Hall, Rochester NY 14627-0221, USA.
[4]US Geological Survey, 345 Middlefield Road, Menlo Park CA 94025, USA.

Initial receipt: 30 January 2006
Acceptance: 19 May 2006
Web publication: 23 June 2006
Ms 197SR-001

A PALEOLATITUDE TEST OF HAWAIIAN HOTSPOT MOTION

The Hawaiian-Emperor volcanic chain is an iconic feature that appears in most introductory Earth science textbooks as the case example of age-progressive volcanism recording plate motion over a sublithospheric hotspot. The westward increase in island age, evident from volcano morphology, was recognized by the first native peoples and remarked upon by the first visiting naturalists (Darwin, 1842; Dana, 1849). With the successful application of the K-Ar method to some of the earliest age determinations on basaltic rocks (McDougall, 1964), a monotonic westward aging of the Hawaiian volcanoes was confirmed.

Wilson (1963) first noted the utility of the orientation of the Hawaiian-Emperor lineament and the rate of migration of volcanic activity along it as a reference frame for Pacific plate motion over a hotspot embedded in the mantle. Following the proposition that the Hawaiian hotspot is stationary, which is seemingly supported by the congruent geometries of several Pacific hotspot-related lineaments, Morgan (1971) proposed that Pacific plate motion could be quantified by a set of stage rotations fitting the hotspot volcanic trails, with angular velocities determined from radiometric ages of rocks sampled from the volcanoes. The great longevity of some of the volcanic trails (>100 m.y.) was ascribed to whole-mantle, upwardly convecting, narrow plumes that maintain a constant delivery of warmer-than-ambient mantle to the hotspots (Morgan, 1971).

Shortly thereafter, however, the fixed hotspot hypothesis was challenged. Given that plate tectonics is the expression of a convecting mantle, it is reasonable that any persistent feature embedded in the mantle, like a plume-fed hotspot, should also be moving with respect to other parts of the mantle and the spin axis. Analyses of global plate circuits suggested large relative motions between Hawaii and hotspots in the Atlantic and Indian Oceans (Molnar and Atwater, 1973). Subsequent studies have supported the results of these early plate circuit tests (Molnar and Stock, 1987; Cande et al., 1995; Norton, 1995; DiVenere and Kent, 1999; Raymond et al., 2000; Steinberger et al., 2004). Uncertainties in the plate circuits (e.g., potential motion between East and West Antarctica and tectonic complexities associated with the final transfer to the Pacific plate) have limited a general acceptance of these conclusions.

The important question, from the point of view of a useful frame of reference for plate motions, is the magnitude and constancy of this hotspot motion. An alternative approach to examine hotspot fixity is to determine the age and paleolatitude of volcanoes that form a given hotspot track. For the Hawaiian hotspot, the paleolatitudes of extinct volcanic edifices of the Emperor chain should match the present-day latitude of Hawaii (~19°N) if the hotspot has remained fixed with respect to Earth's spin axis.

Previous paleolatitude estimates for Pacific Basin sites have been based on remote sensing data (modeling of marine magnetic anomalies of seamounts observed during magnetic surveys and of the skewness of marine magnetic anomalies). These analyses provided early important clues to Pacific plate motion. Whereas remote sensing data are still used in a few studies (e.g., Harada and Hamano, 2000), it is generally accepted that such data lack the resolution to address modern questions on hotspot motion (DiVenere and Kent, 1999). Instead, the most reli-

able indicators of paleolatitude are basaltic rocks, but enough time must be spanned by any section such that geomagnetic secular variation is sampled.

Recovery of such samples requires ocean drilling technology, specifically that available in the Ocean Drilling Program (ODP) and its predecessor program (the Deep Sea Drilling Project [DSDP]).

Paleomagnetic data provide estimates of motion relative to Earth's spin axis. A variable that must be considered in the interpretation of paleomagnetic data is the potential shift of Earth with respect to the spin axis, a process known as polar wander (Goldreich and Toomre, 1969). Addressing this variable is in fact directly related to the issue of hotspot motion: modern estimates of polar motion have been based on analyses of paleomagnetic data viewed in a fixed hotspot reference frame. The motion derived from this calculation is often called "true polar wander" (TPW) (e.g., Besse and Courtillot, 2002). Prior attempts to define TPW have largely been based on paleomagnetic data from the Atlantic-bordering continents. The availability of new paleomagnetic data sets from oceanic drilling of seamounts in the Pacific Ocean basin during the early 1990s provided an opportunity to test such models. The new paleomagnetic data conflicted with existing TPW models and instead indicated relative motion between Pacific hotspots and those in the Indo-Atlantic realm (Tarduno and Gee, 1995). Subsequent analyses of the continental record indicated only minor post-Cretaceous polar wander (Tarduno and Smirnov, 2001, 2002).

The prior work on plate circuits, the failure of TPW to explain Pacific paleomagnetic data, and the inferences on hotspot motion stemming from these analyses set the stage for additional work. Specifically, the desire to obtain a new and more extensive Pacific data to test hotspot motion motivated ODP Proposal 523 (J.A. Tarduno, R.D. Cottrell, and B. Steinberger, Motion of the Hawaiian Hotspot during Formation of the Emperor Seamounts: A Paleomagnetic Test [**earth.rochester.edu/pmag/odp-proposal523.html**]). The study proposed eventually became ODP Leg 197.

Below, we review the paleomagnetic results from Leg 197, as well as the geophysical survey profiles that were essential for site selection; these data, together with the geochronological results (Duncan and Keller, 2004), form the basis for the hotspot motion test. We follow this description with a brief summary of other work related to hotspots that has followed Leg 197. In addition, data bearing on the long-term history of the geodynamo resulting from analyses of Leg 197 cores are also reviewed. These data, together with the results of the hotspot motion test, provide new insight into the nature of large-scale mantle convection. A companion program of Leg 197 drilling was to describe the volcanic development and geochemical variability within the Emperor Seamounts, compared with the Hawaiian Islands, in order to assess the effect of changing lithospheric thickness and the contributions of mantle plume and oceanic lithosphere to melting throughout the history of the Hawaiian hotspot. This program is also briefly summarized.

The reader is referred to additional reports of biostratigraphic studies (**Bordine et al., Siesser,** and **Tremolada and Siesser,** all this volume) and logging (**Gaillot et al.,** this volume), which we do not review.

Paleomagnetic Results from Leg 197

Prior paleomagnetic analyses of 81-m.y.-old basalt recovered from the Emperor Seamounts (Detroit Seamount, ODP Site 884) yielded a

paleolatitude of ~36°N (Tarduno and Cottrell, 1997), clearly discordant with the latitude of Hawaii. Only one other data set that averaged secular variation was available prior to Leg 197. Data from ~61-m.y.-old basalt (Sharp and Clague, 2002) from Suiko Seamount define a paleolatitude of ~27°N (Kono, 1980). Together, these data sets suggest that the Emperor Seamounts record southward motion of the hotspot plume in the mantle (Tarduno and Cottrell, 1997).

Leg 197 sought to test the hypothesis of southward motion of the Hawaiian hotspot by drilling additional basement sites in the Emperor chain (Fig. F1). Detailed stepwise alternating-field (AF) demagnetization data were collected aboard the drillship *JOIDES Resolution* (Tarduno, Duncan, Scholl, et al., 2002). All analyses were conducted on standard paleomagnetic minicores, and directions were fit using principal component analysis. Although these shipboard data are of high resolution, they alone are insufficient to define paleolatitudes. Magnetic minerals with intermediate to high coercivities, carrying magnetizations resistant to AF demagnetization, are commonly formed during subaerial or seafloor weathering. The presence of these minerals, which include titanomaghemite, hematite, and a range of oxyhydroxides, had been inferred on the basis of rock magnetic measurements, and they have been directly observed in some of the recovered lava flow samples using reflected-light microscopy. The magnetizations of these mineral phases are easily resolvable with thermal demagnetization (Doubrovine and Tarduno, 2004a, 2004b). Accordingly, detailed (25°C steps; 50°–625°C range) thermal demagnetization data, measured on a high-resolution 2G Enterprises SQUID (super-conducting interference device) magnetometer, were collected as part of Leg 197 postcruise work.

At least several millennia of geomagnetic field behavior must be sampled such that the axial dipole term becomes dominant, allowing a statistically significant estimate of the paleolatitude. The angular dispersion of inclination averages (McFadden and Reid, 1982) from independent lava flows (inclination groups) were compared with global lava data of the same age (McFadden et al., 1991) to examine whether secular variation had been adequately sampled (Cox, 1970; Brock, 1971). Analyses of the Leg 197 data utilized observations of the physical aspects of the lava flows, as well as petrologic and geochemical data, to group cooling units into lava units. This approach has resulted in a more conservative assignment of inclinations groups than used in prior studies.

Marine sediments can also provide useful paleolatitude information, but the results must be interpreted with care; in general, they provide minimum values of paleolatitude because of potential compaction-induced inclination flattening (e.g., Anson and Kodama, 1987; Arason and Levi, 1990; Tarduno, 1990). An advantage magnetizations from sediments have with respect to those from basalt, however, is that they can record significant time intervals. Similarly, chemical remanent magnetization (CRM), carried by minerals formed during weathering, can preserve stable magnetizations that provide insight into the time-averaged field.

Below, we briefly summarize the postcruise thermal demagnetization data collected from each of the Leg 197 sites that were reported in a summary article (Tarduno et al., 2003). We also review more recent rock magnetic analyses.

F1. Leg 197 sites in the Emperor Seamounts, p. 25.

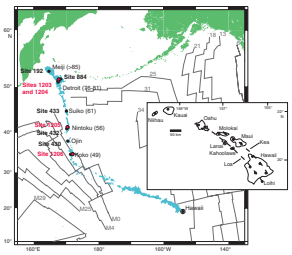

Koko Seamount (Site 1206)

Site 1206 (Fig. F1) was positioned on the southeastern side of the lower summit terrace on Koko Seamount using crossing underway seismic profiles. The central area of Koko Seamount is capped by a relatively thick (~200 m) sequence of sedimentary deposits overlying a plateau of igneous basement. To avoid penetrating the sedimentary cover, which probably includes reefal debris, Site 1206 was positioned over an acoustically imaged sequence of flat-lying lava flows and volcaniclastic beds underlying the thinly sedimented southeast flank of the seamount's summit platform (Kerr et al., this volume). Thin intercalations of limestone, volcaniclastic sandstone, and a deeply weathered flow top were also recovered, providing geological evidence of time between lava flow units.

Plateaus in ^{40}Ar-^{39}Ar incremental heating spectra from six whole-rock samples yield a mean age of 49.15 ± 0.21 Ma (2σ uncertainty quoted; Duncan and Keller, 2004).

Seventeen inclination groups, spanning three polarity zones (Chrons 21n-21r-22n) (Cande and Kent, 1995) were identified in the thermal demagnetization data having a mean inclination (I_t = 38.3° +6.9°/–9.3°; hereafter all uncertainty regions are 95% confidence interval unless otherwise noted), nearly identical to that isolated by AF treatment (I_{af} = 38.5° +8.4°/–10.9°, based on 14 inclination groups sampled) (Fig. F2). The angular dispersion of the thermal data (S_f = 15.3° +4.3°/–2.7°) is within error of that predicted by global 45- to 80-Ma lava flows (McFadden et al., 1991). Comparison of the inclination units based on thermal demagnetization with a synthetic Fisher (Fisher, 1953) distribution (Fig. F2) suggests that the basalt sequence represents well the time-averaged geomagnetic field. Furthermore, a highly stable magnetization carried by hematite (likely a CRM with unblocking temperatures >580°C) in samples of the deeply weathered basalt yields a mean inclination that is indistinguishable from that of the lava flows.

F2. Paleomagnetic inclination groups, p. 26.

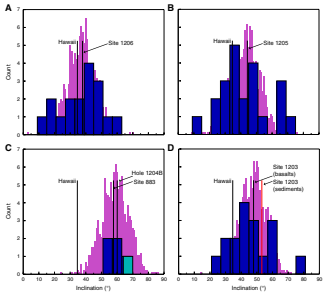

Nintoku Seamount (Site 1205)

At Site 1205 on Nintoku Seamount (Fig. F1), a sequence of 25 subaerially erupted a'a and pahoehoe lavas and interbedded sediment and soil horizons were recovered in 283 m of basement penetration. Two different types of igneous basement produce distinctly different seismic signatures in the vicinity of Site 1205 (Kerr et al., this volume). The upper unit is imaged as laterally coherent, low frequency, and west-dipping reflections that coincide with a bowl-shaped sequence of dominantly alkalic basalt lava flow units interbedded with soil layers. The lower acoustic unit at the base of the drilled section is more acoustically massive and rises gently upward to the southeast. The strongly reflective sequence of lava flows and soil interbeds of the upper acoustic unit thins in this direction. The more massive acoustic character of the lower unit is linked to the less common occurrence of soil horizons below ~203 meters below seafloor (mbsf). Plateaus in ^{40}Ar-^{39}Ar incremental heating spectra from six whole-rock basalt samples spanning the section give a mean age of 55.59 ± 0.25 Ma (Duncan and Keller, 2004). The thermal demagnetization data (22 inclination groups) yielded a mean (I_t = –44.3° +10.3°/–6.3°) that is similar to that of the AF data (I_{af} = –45.7° +10.5°/–6.3°). The estimated angular dispersion of the thermal data (S_f = 19.9° +4.8°/–3.2°) is higher than predicted by models based on average data from 45- to 80-Ma lavas (McFadden et al., 1991)

and may point to higher-frequency changes in secular variation with time. Nevertheless, the geologic evidence for time, together with a comparison of the data versus a Fisherian distribution (Fig. F2), suggests the mean value represents the time-averaged field.

Detroit Seamount (Site 1204)

Two holes were drilled at Site 1204 on Detroit Seamount (Holes 1204A and 1204B), penetrating 60 and 138.5 m of basalt, respectively. Detroit Seamount, one of the northernmost volcanic edifices of the Emperor Seamount chain, is a broad volcanic plateau constructed of little deformed but locally faulted basement of lava and volcaniclastic beds. Flows and volcaniclastic units are distinguishable on the seismic records. Basement is overlain by a capping of drift sediment, the Meiji Drift, as thick as 800–900 m. Detailed descriptions of the seismic data used to position Leg 197 drilling sites in nonstructural settings are provided in Kerr et al. (2005). Diamictite and volcanic ash–rich sediment directly overlying basement contain nannofossils of Campanian age (CC22–CC23, ~73–76 Ma) (Berggren et al., 1995); nannofossils of this zone were also recovered in a sediment interbed in the last core from Hole 1204B, suggesting the entire basement section drilled is of this age.

Reflected-light microscopy showed a dominance of titanomaghemite in basalt samples. Approximately 30% of the samples examined failed to show a simple AF demagnetization behavior; instead, the presence of at least one unresolved magnetic component was suggested. Thermal demagnetization revealed a clear two-component structure in many samples. A reversed polarity component was defined at low unblocking temperatures (~100° to 275°–350°C), whereas a normal polarity component was defined at higher temperatures. Because of this unusual behavior, a detailed investigation of the Site 1204 basalts was conducted (Doubrovine and Tarduno, 2004a).

Extensive rock magnetic tests coupled with X-ray diffraction (XRD) and scanning electron microscopy (SEM) characterization established that the lower unblocking temperature component in the Site 1204 basalts (as well as those from ODP Site 883) represents a partial self-reversal of the primary magnetization. Self-reversal of natural remanent magnetization, the remarkable ability of some rocks to acquire a magnetization antiparallel to that of Earth's geomagnetic field, has been established in only a few, arguably rare, igneous rocks bearing hemoilmenite. However, hemoilmenite is absent from the Site 1204 rocks. Instead, the self-reversed component is carried by titanomaghemite, which formed by in situ low-temperature oxidation; the self-reversal process is consistent with ionic reordering as described by Verhoogen (1956, 1962). Subsequent measurements of basalt from other sites seem to suggest that the "self-reversing" compositional field is even more restrictive than that envisioned in the classic work of Verhoogen (1956, 1962) and O'Reilly and Banerjee (1966). When present, self-reversal in titanomaghemite connotes extreme oxidation at low temperature (needed to maintain the cation-deficient structure of titanomaghemite) (Doubrovine and Tarduno, 2005). This could be achieved through sustained fluid flow and Fe removal; therefore, self-reversals may provide one way of identifying such processes in oceanic crust.

Because the self-reversed component is not typically isolated by AF demagnetization, we exclude from consideration paleomagnetic results

based on AF results from Detroit Seamount, including a study in which the two-component magnetic structure was missed (e.g., Sager, 2002). Instead, we restrict our analysis to the high unblocking temperature magnetization. Although carried by titanomaghemite, it is nevertheless this magnetization that best reflects the primary field direction (see additional discussion in Doubrovine and Tarduno, 2004b).

Only a single inclination unit was identified in Hole 1204A, with a mean inclination I_t = 64.5° +10.2°/–19.0°. On the basis of the lithofacies succession in Hole 1204B, five inclination groups were identified. Thermal demagnetization results indicate a mean inclination of (I_t =) 60.1° +5.2°/–5.5°. Angular dispersion estimates are low (S_f = 3.1° +2.0°/–0.9°) and at face value suggest that the sequence does not adequately sample secular variation. However, thermal demagnetization data from samples of a breccia interbedded with the lavas show a consistent direction, similar to that of the basalt flows. This observation, together with the presence of titanomaghemite, suggests that CRMs acquired over time might be important at Site 1204.

Detroit Seamount (Site 1203)

Eighteen compound lava flow units and 14 volcaniclastic sedimentary interbeds were drilled in 453 m of basement penetration at Site 1203 on Detroit Seamount. Plateaus in ^{40}Ar-^{39}Ar incremental heating spectra from three whole-rock basalt samples and two feldspar separates yield a mean age of 75.82 ± 0.62 Ma (Duncan and Keller, 2004). Thermal demagnetization of the two uppermost pillow basalt flows of the sequence revealed a two-component structure similar to that observed at Site 1204. In all other basalt samples, a simple univectorial decay was observed after the removal of minor overprints. The thermal demagnetization results (16 inclination groups) yield a mean (I_t = 48.6° +7.0°/–10.6°) similar to that calculated from AF data (I_{af} = 50.0° +7.3°/–10.6°, for 14 inclination units). The estimated angular dispersion of the thermal demagnetization data (S_f =18.4° +6.9°/–3.7°) is slightly higher than that expected from global lava flow data (McFadden et al., 1991).

Paleolatitude History

The inclination groups, averaged by site, form a time-progressive sequence of decreasing paleolatitude with time (Fig. F3). This is inconsistent with the fixed-hotspot hypothesis and instead indicates the plume was moving with respect to the spin axis. Whereas many scientists believe that long-standing nondipole terms are insignificant in the geomagnetic field during the last 200 m.y. (Courtillot and Besse, 2004), it should be noted that if the one model calling for minor octupole fields is correct (Van der Voo and Torsvik, 2001), our paleolatitude data would underestimate the true rate of hotspot migration. As discussed earlier, polar wander, the rotation of the entire solid Earth with respect to the spin axis (Goldreich and Toomre, 1969), is an alternative physical mechanism that might explain paleolatitude trends. However, polar wander can be tested by examining globally distributed data, and these tests have failed to confirm it (Tarduno and Gee, 1995; Cottrell and Tarduno, 2000b; Tarduno and Smirnov, 2001, 2002; Torsvik et al., 2002; Besse and Courtillot, 2002).

Paleolatitude estimates for Detroit Seamount are available from lava flows and sediments, based on thermal demagnetization. Lava emplace-

F3. Paleolatitude data, p. 27.

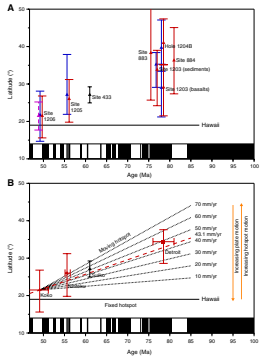

ment was probably less frequent at Site 884 relative to the other sites because it is on the flank of Detroit Seamount. Hole 1204B lavas clearly reflect low angular dispersion, as do the basalts at Site 883 (Doubrovine and Tarduno, 2004b). However, these rocks might carry a CRM acquired over a time interval longer than that of a cooling lava flow, explaining the agreement of their mean inclination with that of the Site 884 basalt section and the Site 1203 sediments. In fact, the mean inclination from the Site 1203 sediments should be a minimum because of potential inclination shallowing. These comparisons further suggest that the mean inclination derived from the basalts at the same site is shallower because the available lavas underrepresent higher inclination values.

Tarduno et al. (2003) presented two averaging scenarios for the Detroit Seamount paleomagnetic data. In one, the paleomagnetic results from the Site 884 basalts, Hole 1204B basalts, and Site 1203 sediments best represent the field estimate (paleolatitude Model A). In another, all the individual basalt inclinations were combined to form a grand mean. Both averaging models indicate high average rates of motion (Model A = 57.7 ± 19.2 mm/yr; Model B = 43.1 ± 22.6 mm/yr) consistent with the hypothesis that the Hawaiian hotspot moved rapidly southward from 81 to 47 Ma. The higher rate of southward motion is in slightly better agreement with the estimates of hotspot motion based on independent relative plate motions (e.g., Raymond et al., 2000), and Doubrovine and Tarduno (2004b) further discuss reasons why the higher-latitude mean value from Detroit Seamount may be accurate. Nevertheless, it is not possible to distinguish between these models with the presently available data. The slow latitudinal plate motion at this time is consistent with plate tectonic driving forces (Cottrell and Tarduno, 2003). The paleomagnetic data are also consistent with geodynamic models of the interaction of a plume with large-scale mantle flow (Steinberger and O'Connell, 1998; Tarduno et al., 2003; Steinberger et al., 2004) (Fig. F4).

F4. Leg 197 vs. geodynamic model results, p. 28.

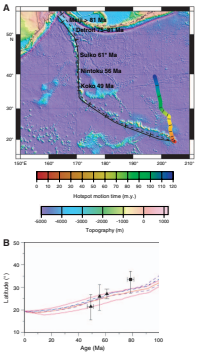

Developments after Leg 197

Following the development of ODP Proposal 523 and publication of the Leg 197 *Initial Results*, several important studies concerning hotspot motion appeared in the literature. Antretter et al. (2002) studied the paleomagnetism of basalt cores recovered from Kerguelen Plateau (ODP Leg 183). The authors concluded that the data supported motion of the Kerguelen hotspot, consistent with geodynamic models of mantle flow. Paleomagnetic analyses of lavas drilled on Ontong Java Plateau during ODP Leg 192 defined a difference between observed paleolatitudes and those predicted by fixed hotspots (Riisager et al., 2003a). These data are consistent with hotspot motion as defined in studies of other Cretaceous Pacific sites (Tarduno and Gee, 1995) and the Emperor Seamounts (Tarduno and Cottrell, 1997). Moore et al. (2004) and Pares and Moore (2005) present detailed analyses of equatorial crossing data based on Pacific DSDP and ODP sedimentary cores. They conclude that the Hawaiian hotspot moved southward since 53 Ma, consistent with Leg 197 results.

Torsvik et al. (2002) review the debate over rapid Cretaceous TPW (Prevot et al., 2000; Camps et al., 2002) vs. hotspot motion (Tarduno and Smirnov, 2001, 2002) and find little evidence for TPW. Courtillot et al. (2003) use Leg 197 results in a comparison of Pacific and Indo-Atlantic paleomagnetic data relative to hotspots in the respective hemispheres. They conclude that there were significant differences between

the two data sets, which by definition cannot be explained by TPW (i.e., rotation of the entire Earth with respect to the spin axis). This result supersedes earlier conclusions reached by Besse and Courtillot (2002) and confirms an earlier finding of relative motion between groups of Pacific and Atlantic hotspots (Tarduno and Gee, 1995). An alternative plate circuit has been recently suggested that invokes a path through the Lord Howe Rise (Steinberger et al., 2004). This plate path also predicts hotspot motion consistent with that defined by the Leg 197 paleomagnetic data.

Koppers and Staudigel (2005) examine the ages of purported hotspot tracks of the central Pacific. They conclude that bends in these tracks, typically taken to be coeval with the Hawaiian-Emperor bend, are in fact of differing age. They offer several explanations, including motion between hotspots within the Pacific Basin and strong lithospheric control on the expression of some hotspot magmatism. For some apparent hotspot tracks this can be taken as support for nonplume models that relate volcanism to extension. The results of Koppers and Staudigel (2005) highlight that attempts at backtracking based on geometry alone, including "hotspotting" (Wessel and Kroenke, 1997, 1998; Wessel and Lyons, 1997; Kroenke et al., 2004), cannot be used to test hotspot motion; instead they must be combined with accurate and complete age information.

The nature of mantle plumes has recently been the subject of numerous debates at meetings and in the literature (e.g., Foulger and Natland, 2003; Sleep, 2003). Some workers see different categories of plumes with different sources within the mantle (e.g., Courtillot et al., 2003). Some recent tomographic investigations have also been interpreted as representing a variety of mantle plumes (Montelli et al., 2004), but the interpretations have sometimes differed from other classifications. Others hold to an interpretation that sees no role for lower mantle plumes (Anderson, 2000, 2004). Whereas the resolution of the tomographic images is itself the subject of lively debate at meetings, it seems likely that the approach will eventually yield conclusive results. Regardless of the possibility of different hotspot types, at the time of the writing of this report no viable alternative exists to the mantle plume model that explains all the data available from the Hawaiian-Emperor chain.

Geomagnetism

Another goal of Leg 197 was to better define characteristics of the Late Cretaceous–Paleogene geomagnetic field. A particular focus was on past field strength, or paleointensity. Several postcruise efforts have been devoted toward that end, using various natural materials recovered during Leg 197.

Whole-Rock Basalt Studies

A classic approach to paleointensity study is to analyze whole-rock basalt samples. A sample's natural remanent magnetization (NRM) is demagnetized over a given temperature range in a zero-field environment. Next, the sample is reheated to the same temperature in the presence of a known laboratory field. As a result, a thermoremanent magnetization (TRM) is imparted to the sample. Given the NRM lost, TRM gained, and applied field, the paleointensity can be calculated. This approach is attributed to Thellier and Thellier (1959), as modified

by Coe (1967), and it is arguably the most rigorous experimental method for the collection of paleointensity data.

The rock magnetic requirements for Thellier paleointensity analysis, however, are severe. The magnetic carriers must be extremely fine grained (having single-domain behavior), they must carry an original TRM, and they must not alter during the Thellier experiments. Carvallo et al. (2004a, 2004b) applied rock magnetic tests on many Leg 197 lavas, seeking samples that might meet these criteria. Ultimately, most of the samples that showed indications of suitable fine magnetic grain sizes (and associated domain states) also showed that the magnetic minerals had undergone some low-temperature oxidation (i.e., much less severe than that displayed by some Site 1204 basalts but still detectable). Under normal seafloor conditions, original titanomagnetite can be partially converted to titanomaghemite (therefore the process is also often called "maghemitization"). Evidence of maghemitization was observed in reflected-light microscopy studies of the Leg 197 lavas (analyses by Clive Neal, reported in Tarduno, Duncan, Scholl, et al., 2002). Maghemitization transforms a TRM into a chemical remanent (or crystallization remanent) magnetization. The accuracy of CRM in recording past field strength is unclear, but it is generally accepted that the process is less efficient than TRM (Dunlop and Ozdemir, 1997; Smirnov and Tarduno, 2005). Submarine basaltic rocks affected by low-temperature magnetization are thought to yield anomalously low paleointensity data (e.g., Gromme et al., 1979).

Carvallo et al. (2004a, 2004b) identified only one lava unit that had apparently escaped the more dramatic effects of low-temperature oxidation. Thellier experiments of these samples yield field strengths ranging from 34.2 to 39.4 µT. These results alone cannot constrain geomagnetic field behavior because they do not span a period sufficient to yield time-averaged field behavior. Nevertheless, as discussed below, the Carvallo et al. (2004a, 2004b) study provides key data for the evaluation of new paleointensity approaches and for understanding the veracity of existing data in the paleointensity database.

Submarine Basaltic Glass

It has been argued that submarine basaltic glass can be a high-resolution recorder of past field strength; the magnetization is thought to be carried by fine-grained magnetic particles within the glass. Because these particles are so Fe rich, questions have been raised about the process of magnetization. Some authors favor a low-temperature CRM process (e.g., Heller et al., 2002; Goguitchaichvili et al., 2004) as opposed to a thermoremanent magnetization; in this case, submarine basaltic glass would not meet the basic requirements for Thellier paleointensity analysis. On the other hand, support for the accuracy comes from studies that show that young submarine glass generally yields field values that agree with known modern field strengths (Pick and Tauxe, 1993).

Time-averaged results are not available from most of the submarine basaltic database (Selkin and Tauxe, 2000). Nevertheless, these data are generally of high technical quality.

Recently, relatively high paleointensity values have been reported from submarine basaltic glass samples of one locality (Troodos ophiolite) formed during the Cretaceous Normal Polarity Superchron (Tauxe and Staudigel, 2004). These have been interpreted as reflecting a higher field strength during the Cretaceous Normal Polarity Superchron, superseding prior interpretations based on submarine basaltic glass that

the Superchron field was of normal or weak intensity (Pick and Tauxe, 1993). Notwithstanding these data, the aggregate of individual sample results available from submarine basaltic glass from the 10- to 160-Ma interval suggest a weak mean field strength for the last 160 m.y. that is close to half the present-day field value (Tarduno and Smirnov, 2004).

Submarine basaltic glass was recovered at a few Leg 197 sites, especially Site 1203 on Detroit Seamount. Smirnov and Tarduno (2003) sought to evaluate the accuracy of this glass as a paleointensity recorder through a rock magnetic, transmission electron microscope, and paleointensity study. They observe neocrystallization of magnetite in Thellier heatings of submarine basaltic glass from three other Cretaceous ODP sites. This alteration resulted in artificially low paleointensity values (Fig. F5). Glasses are thermodynamically unstable; with time and/or increased temperature, they become crystalline. The chemical bonds in glass break over a temperature transitional range (Bouska, 1993; Donth, 2001), and this range overlaps with temperatures applied during typical Thellier experiments. Therefore, the tendency of older submarine basaltic glass to record lower and more variable paleointensity values could reflect subtle experimental alteration, enhanced by natural weakening of bonds and hydration with age, lowering the glass transition temperature.

Smirnov and Tarduno (2003) suggest that monitor samples (i.e., splits of the submarine basaltic glass specimens) be used during the Thellier experiments. Specifically, Smirnov and Tarduno (2003) advocate the use of magnetic hysteresis measurements on the monitor samples after each heating. This experimental approach was adopted by Riisager et al. (2003b) in a study of submarine basaltic glass from Ontong Java Plateau (Leg 192). Experimentally induced alteration similar to that objected from Site 1203 was reported, further suggesting that this could be a general characteristic of older submarine basaltic glass.

F5. Paleointensity data from submarine basaltic glass, p. 29.

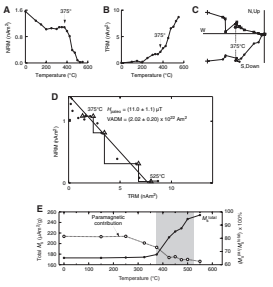

Plagioclase Feldspar Studies and Long-Term Field Behavior

Single plagioclase crystals can contain minute magnetic inclusions (often 50–350 nm) that are shielded by the silicate matrix and less susceptible to natural and experimental alteration (e.g., Smirnov et al., 2003). Thellier paleointensity analyses of plagioclase crystals separated from a modern lava flow on Kilauea, Hawaii, provide a benchmark for this approach (Cottrell and Tarduno, 1999). In that study, paleointensity values were obtained that matched the field value known from magnetic observatory data.

Many of the lavas from Nintoku Seamount Site 1205 contained plagioclase feldspar potentially suitable for Thellier analyses. To test the potential of these crystals, Tarduno and Cottrell (2005) conducted several rock magnetic tests, including the measurement of first-order reversal curves (FORCs) (Pike et al., 1999; Roberts et al., 2000). In a FORC diagram the horizontal axis (*H*c) is a gauge of microcoercivity, whereas the vertical axis (*H*b) is a measure of the interaction field between magnetic grains. Neither the whole rocks nor the single crystals from Site 1205 show evidence for large magnetic interactions (Fig. F6). But the plagioclase FORC distributions are clearly more favorable for paleointensity studies. The whole-rock FORC diagrams and individual magnetic hysteresis curves show evidence for very low microcoercivities, consistent with the presence of multidomain grains. Such grains violate Thellier requirements (e.g., Dunlop and Ozdemir, 1997; Dunlop et al., 2005).

F6. First-order reversal curve, p. 30.

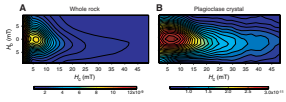

NRM/TRM data from 44 of 86 plagioclase crystals measured from 11 lava flow units from Site 1205 that meet experimental reliability criteria (Cottrell and Tarduno, 2000a; Tarduno and Cottrell, 2005) yield a mean field value of 42.8 ± 13.6 μT (1σ uncertainty) (Fig. F7). Plagioclase crystals large enough for paleointensity analyses are not available from the one aphyric lava for which Carvallo et al. (2004a) obtained Thellier paleointensity data seemingly unaffected by low-temperature oxidation. But the range of paleointensity values obtained from the whole rocks (34.2–39.4 μT) is compatible with that available from the plagioclase crystals from the Site 1205 sequence.

Perhaps more importantly, Carvallo et al. (2004a) also performed Thellier experiments on some Site 1205 lavas that had undergone low-temperature oxidation. Interestingly, these yielded nominal whole-rock paleointensity values lower than those obtained using plagioclase crystals from the same units (Tarduno and Cottrell, 2005). This observation is consistent with the hypothesis that low-temperature oxidation and the acquisition of CRM has led to a low field bias in the paleointensity database from whole rocks (Tarduno and Smirnov, 2004).

The plagioclase crystals come from lavas that span the basement sequence. We can be confident that time elapsed between the lavas because some lava tops are deeply weathered, whereas in other cases, soil horizons separate the lavas (Tarduno, Duncan, Scholl, et al., 2002). Paleomagnetic directions from whole rocks and their associated estimate of angular dispersion (Tarduno et al., 2003) further indicate that the flows are independent in time and average secular variation. Thus, the virtual dipole moments obtained from each lava flow together comprise a time-averaged paleomagnetic dipole moment. This moment, 8.9 × 10^{22} A-m² (Tarduno and Cottrell, 2005), is significantly weaker (at the 95% confidence level) than those derived from plagioclase crystals from Cretaceous Normal Polarity Superchron lavas (Cottrell and Tarduno, 2000a; Tarduno et al., 2001, 2002). The standard deviation of the Site 1205 virtual dipole moments (32%) is similar to that of the modern field but nearly three times greater than those recorded by the Cretaceous Normal Polarity Superchron plagioclase crystals (Fig. F8).

Available plagioclase-based paleointensity data now sample the range of field behavior displayed by the geodynamo during the last 200 m.y. The pattern suggested by the ensemble of single-crystal paleointensities traces an inverse relationship between field strength and reversal frequency (Fig. F8), as was suggested in the pioneering work of Cox (1968) (see also discussion by Banerjee, 2001). Such a relationship has also been suggested in some subsequent models (e.g., Larson and Olson, 1991) and analyses of marine magnetic anomaly intensities (McElhinny and Larson, 2003).

There are several competing interpretations of the geomagnetic reversal chronology; it is useful to mention these before discussing further the importance of the Site 1205 paleointensity results. In one interpretation, nonstationary intervals bound the Cretaceous Normal Polarity Superchron (McFadden et al., 1991). In another interpretation, the reversal history is best represented by a series of stationary regimes (Lowrie and Kent, 2004). In still another interpretation, the Cretaceous Normal Polarity Superchron is thought to be part of a nonstationary interval spanning 130–25 Ma, followed by a stationary interval. The last interpretation has particular importance because it has been used to further suggest that superchrons reflect nonlinear dynamo processes (Hulot and Gallet, 2003).

F7. Paleointensity results from plagioclase crystals, p. 31.

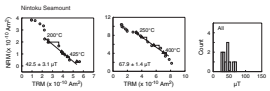

F8. Plagioclase crystals and whole-rock lava results, p. 32.

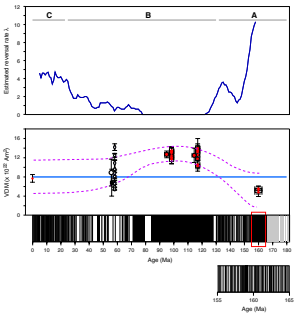

In contrast, superchrons may reflect times when the nature of core/mantle boundary heat flux allows the geodynamo to operate at peak efficiency, as suggested in some numerical models (Glatzmaier et al., 1999; Roberts and Glatzmaier, 2000; Olson and Christensen, 2002; Christensen and Olson, 2003), whereas the succeeding period of reversals may signal a less efficient dynamo with a lower and more variable dipole intensity. This interpretation is consistent with the observations from the Site 1205 plagioclase crystals and the overall plagioclase paleointensity data set (Tarduno and Cottrell, 2005). The timescale for the transition between these states is consistent with an active lower mantle, controlling the nature of the geodynamo.

GEOCHEMICAL VARIABILITY OF THE HAWAIIAN HOTSPOT

Age Distribution of Volcanism

An important development in quantifying hotspot dynamics has been the recent improvement in acquisition of accurate and precise age determinations by ^{40}Ar-^{39}Ar incremental heating methods (Koppers et al., 2000). Many of the radiometric ages published into the 1990s, which have been used to infer the time-space distribution of volcanic activity in prominent chains of islands and seamounts (e.g., Duncan and Clague, 1985), were based on total fusions (one-step heating) or incremental heating experiments on minimally treated, altered whole rocks. As Koppers et al. (2000) have shown, acid-leached crystalline groundmass and mineral separates (usually plagioclase feldspar) from seawater-altered tholeiitic and alkalic basalts often produce much more precise and reproducible plateau and isochron ages from incremental heating age spectra. Ages based on these improved methods often show significant differences from published ages from the same samples (Koppers et al., 2004).

Duncan and Keller (2004) report age determinations from deep drilling samples at three of the Emperor Seamounts (Fig. F1): Detroit (Sites 1203 and 1204), Nintoku (Site 1205), and Koko (Site 1206). Combined with new dating results from Suiko Seamount (DSDP Site 433) and dredged rocks from volcanoes near the prominent Hawaiian-Emperor bend (Sharp and Clague, 2002), the overall trend is increasing volcano age from south to north along the Emperor Seamounts, consistent with the hotspot model. However, there are important departures from the earlier modeled simple linear age progression (Clague and Dalrymple, 1987). Specifically, Pacific plate velocity (relative to the Hawaiian hotspot) was variable, from ~5 cm/yr at the northern end of the Emperor seamounts to ~10 cm/yr at the southern end, decreasing abruptly to ~5 cm/yr after the change in orientation at the bend before increasing again to 9 cm/yr along the Hawaiian Ridge (Fig. F9).

The measured paleolatitude change between Detroit and Koko Seamounts amounts to 4–5 cm/yr southward drift of the Hawaiian hotspot with respect to the geomagnetic pole (Tarduno et al., 2003). The relative motion between the Pacific plate and the hotspot during this time was ~5 cm/yr in a direction defined by the Emperor Seamounts. We must conclude that the Pacific plate showed very little northward motion (relative to the geomagnetic pole) between 81 and 61 Ma.

Koppers et al. (2004) report radiometric ages from a reanalysis of 10 samples from the Watts et al. (1988) study of the Louisville Seamounts

F9. Age distribution of volcanic centers, p. 33.

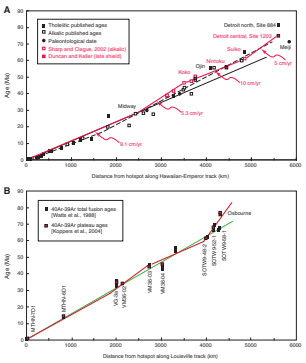

and two new samples. The pattern of northwestward-increasing ages observed by Watts et al. (1988) was confirmed, but rates of migration of volcanism vary considerably along the chain. Ages for seamounts younger than 47 Ma match closely with those of the Watts et al. (1988) study, but plate over hotspot velocities from volcanoes older than 62 Ma are significantly slower than proposed earlier (Fig. F9). Whereas the distribution of age determinations along the Louisville chain is less dense than that for the Hawaiian-Emperor chain, common intervals of faster and slower plate motion relative to the hotspots are apparent. This implies that, while hotspots may drift, the volcanic lineaments can still provide useful information on Pacific plate motion. In fact, Koppers et al. (2004) combined the Steinberger et al. (2004) predicted motion of the Hawaii and Louisville hotspots with an optimized set of Pacific plate stage rotations to closely match the observed geometry and newest age progressions determined for these volcanic chains (Fig. F10).

F10. Computed hotspot motion and tracks, p. 34.

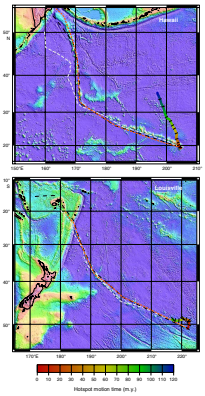

Geochemical Variations

Geochemical, petrological, and physical volcanological studies of the Hawaiian-Emperor volcanic lineament provide information about (1) the chemical and mineralogical character of the mantle source for melting at any given location, (2) long-term variability in the flux and composition of mantle sources for volcano construction, and (3) the geometry and dynamics of mantle melting, melt migration, and evolution through the crustal zone. Our models for Hawaiian volcano development are very much biased toward processes and timescales of activity that can be observed at the young, southeast end of the >80-m.y.-old chain, where the islands record only the last 5 m.y. of hotspot activity. It is of great interest to know whether the older volcanoes of the Hawaiian Ridge and Emperor Seamounts were constructed from the same types of magmas, at similar rates of eruption, and in a similar plate tectonic setting as the Hawaiian Islands or whether there are important changes in the nature of the hotspot or interaction of the Pacific lithosphere and the underlying mantle over the whole of Hawaiian-Emperor lineament construction.

Our current model of Hawaiian volcano development is based on field studies, submarine mapping, and sampling of Loihi Seamount and deep drilling at the Hawaii Scientific Drilling Project site on the island of Hawaii (Fig. F11). Essentially, volcanic activity starts with submarine eruptions of low-volume alkalic lavas, moving to mixed alkalic and tholeiitic lavas with increasing rates of eruption (preshield stage), progressing to dominantly tholeiitic lavas at peak eruption rates (main shield stage), changing to dominantly alkalic lavas with dramatically decreasing eruption rate (postshield stage). The timescale for this construction is on the order of 0.5 m.y. After a quiescent period of several million years, extensional tectonics may allow small-volume, small-degree mantle melts to make their way to the surface and erupt as undersaturated posterosional lavas. An addition to this well-known volcano development model is the finding reported by Kerr et al. (2005) that old volcanoes (Detroit Seamount, 76 m.y.) continued to collapse under extension at least through late Miocene time. Volcanic edifices occur on the summit of this coalesced set of shields that, based on the age of sediments they pierce and ash layers recorded in Leg 197 drilling, must have been active throughout much of the Eocene (~52–34 Ma). Hence, rejuvenescent volcanism resulting from gravitational collapse or regional extension may be possible at any of the Hawaiian volcanoes.

F11. Models of Hawaiian volcano evolution, p. 35.

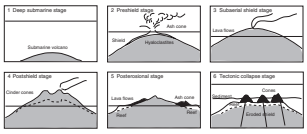

The volcanoes that comprise the islands of Hawaii, Maui, Molokai, Lanai, and Kahoolawe record Hawaiian magmatism over the last 2 m.y. The lavas erupted here span the compositional range observed from all Hawaiian volcanoes over the past 5 m.y. (out to Kauai) and can be related to source end-member compositions for melting (Gaffney et al., 2005). Major and trace element and isotope (Sr, Nd, Pb, Hf, and Os) compositions of shield-stage lavas from these volcanoes are consistent with ancient, recycled oceanic crust and primitive plume material in the mantle source (so-called, Kea-, Koolau- and Loihi-type magmas) (Lassiter and Hauri, 1998; Blichert-Toft et al., 1999; Ren et al., 2005). Gaffney et al. (2005) examine trace element models that include melting of recycled ocean crust (eclogite pods and pelagic sediment) mixed within primitive plume mantle (Koolau type) or melting of recycled ocean crust that has been first fertilized by reaction with partial melts from associated crustal gabbro, without mixing with primitive plume mantle (Kea type). Chen and Frey (1985) propose that Hawaiian postshield-stage lavas were formed by melts from the plume mixing with melts derived from the oceanic lithosphere, which is the wallrock of the melt conduits to the volcanoes. In this view, the contribution from the plume decreases with time (up section) as the plate moves away from the hotspot.

The time and space distribution of the volcano compositions has led to the notion that the Hawaiian plume is concentrically zoned, with Koolau- and Loihi-type volcanoes over the core of the plume and Kea-type volcanoes over the edge of the plume (Hauri, 1996; Lassiter and Hauri, 1998; DePaolo et al., 2001) (Fig. **F1**). Compositional heterogeneity in the Hawaiian hotspot exists, then, at many scales, yet there is evidence that the full range and pattern of variability may persist for very long periods (>5 m.y.). Deep sampling of the Emperor Seamounts provides the means to examine the range and scale of compositional variability of the Hawaiian hotspot over much longer periods (>80 m.y.) and through changes in plate tectonic setting (near-spreading ridge to midplate). The sections of lava flows sampled during Leg 197 drilling are also significantly longer than earlier sampling by dredging or drilling (with the exception of DSDP drilling at Suiko Seamount) and provide considerable detail about short-term changes in lava composition and volcanic processes. Observations of lava flow thickness, vesicularity, crystallinity, and morphology, together with analysis of volcanic sediment, have provided a picture of eruptions in subaerial to shallow-water conditions at Detroit and Koko Seamounts and waning subaerial activity at Nintoku Seamount (Fig. **F12**). Combining petrological and geochemical data with such physical volcanological observations leads to interpretation of volcanic stages within the Hawaiian volcano development model for cored samples from the Emperor Seamounts.

Major and trace element compositions for basaltic rocks cored during Leg 197 conform closely with compositions known from the Hawaiian volcanoes (Fig. **F13**). Detroit seamount lavas range from alkalic to tholeiitic compositions, consistent with preshield to main-shield stages; Nintoku Seamount lavas are dominantly alkalic compositions, consistent with waning postshield stage; Koko Seamount lavas are dominantly tholeiitic compositions, consistent with main-shield stage eruptions. Schafer et al. (2005) report major and trace element and Sr and Nd isotopic compositions for alkalic, postshield stage lavas cored at Site 1205, Nintoku Seamount (~56 m.y.). These are similar to those of young, postshield stage lavas from the Hawaiian Islands. A modified version of the Chen and Frey (1985) model for postshield stage lavas, in

F12. Volcano environment, p. 36.

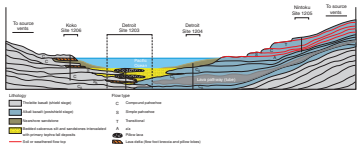

F13. Major element variability for Hawaii vs. Emperor Seamount lavas, p. 37.

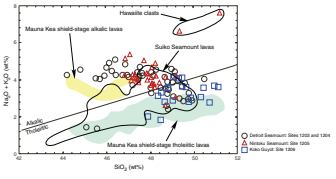

which the Pacific Ocean lithosphere, previously metasomatized by small-degree upper mantle melts, is mixed with melts from the Hawaiian plume mantle appears to explain the trace element and isotopic compositions of the Nintoku Seamount lavas without the need to invoke unreasonably small degrees of mantle melting.

Huang et al. (2005) report major and trace element and isotopic compositions for lava flows from Detroit Seamount (76-81 m.y.), one of the oldest existing Hawaiian volcanic systems, now cored at six locations. Tholeiitic basalts on the eastern flank and alkalic basalts on the summit plateau have been identified. At summit Site 1203 subaerial pahoehoe alkalic lavas occur beneath submarine-erupted tholeiitic lavas, indicating a possible preshield–shield stage transition. The surprising upward change from subaerial to submarine eruption conditions implies rapid subsidence of the volcano, consistent with an inferred near-spreading ridge setting of the seamount at ~80 m.y. Such an interpretation is supported by the lack of age difference between the youngest lavas and oldest sediments at this site. A shallower depth of melt segregation for Detroit Seamount lavas relative to Hawaiian Island lavas is also consistent with construction on thinner oceanic lithosphere (near ridge axis). Huang et al. (2005) confirm the previously reported decrease in $^{87}Sr/^{86}Sr$ for shield lavas northward along the Emperor Seamounts (Keller et al., 2000). Indeed, tholeiitic lavas from Detroit Seamount have the most extreme isotopic composition within the Emperor seamounts, and overlap the $^{87}Sr/^{86}Sr$–$^{143}Nd/^{144}Nd$ field for Pacific mid-ocean ridge basalt (MORB). However, in contrast to Pacific MORB, Detroit Seamount lavas trend to extremely unradiogenic Pb isotopic compositions (Fig. **F14**) and contain relatively high Ba/Th that is characteristic of Hawaiian Island lavas. Huang et al. (2005) conclude that Detroit Seamount lavas sample an intrinsic component present in the Hawaiian hotspot for at least 81 m.y.

Frey et al. (2005) focus their attention on the Hf isotopic composition of the geochemically depleted component in Hawaiian-Emperor lineament lavas. As noted earlier, the Chen and Frey (1985) model recognizes the involvement of old oceanic lithosphere in producing characteristics of the postshield stage lavas in Hawaiian volcanoes. The most depleted shield-stage lavas at Detroit Seamount have many similarities to Pacific MORB, but important differences exist, namely the trends to relatively unradiogenic Pb isotopic compositions (Huang et al., 2005) and steep trends of $^{176}Hf/^{177}Hf$ vs. $^{143}Nd/^{144}Nd$. Frey et al. (2005) propose that a depleted component, intrinsic to the hotspot, has contributed to these shield-stage lavas throughout the Hawaiian-Emperor lineament and is a persistent feature of the long-lived plume (Fig. **F15**).

Keller et al. (2004) measured He isotopic compositions in olivines from picrites and basalts from the Hawaiian-Emperor lineament and report that high $^{3}He/^{4}He$ is a persistent characteristic of the hotspot for its entire history. Picrites erupted at 76 m.y. at Detroit Seamount have $^{3}He/^{4}He$ ratios at the lower end of the range for the Hawaiian Islands but still above the range of modern MORB. During this time volcanism occurred on thin oceanic lithosphere close to a spreading ridge and produced lava compositions that, except for the elevated He and low Pb isotopic compositions, would be indistinguishable from Pacific MORB. The $^{3}He/^{4}He$ of Hawaiian-Emperor volcano lavas increased dramatically during the Late Cretaceous as the distance between the spreading ridge and the Hawaiian hotspot increased (Fig. **F15**). The $^{3}He/^{4}He$ isotopic composition of shield lavas stabilized at high values by 61 m.y. (Suiko

F14. Nd and Pb isotopic variability, p. 38.

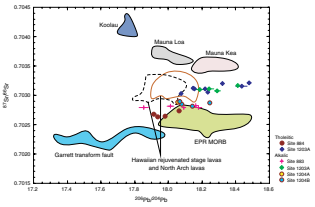

F15. Isotopic variability along Hawaiian-Emperor volcanic lineament, p. 39.

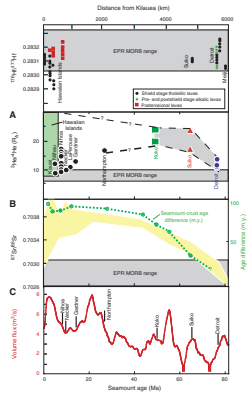

Seamount), while trace element and Sr isotopic compositions continued to change before arriving at ~45 m.y. at values similar to those of the Hawaiian Islands. The contribution of the plume component to Hawaiian-Emperor chain volcanoes is therefore more sensitively recorded by $^3He/^4He$ than by other geochemical indicators through the Emperor Seamount phase of hotspot activity. A poor correlation between $^3He/^4He$ and calculated plume flux based on bathymetry and residual gravity anomalies (Van Ark and Lin, 2004) suggests that variations in delivery of primitive plume mantle does not control the total flux of hotspot melting.

SUMMARY

The results of the Leg 197 paleomagnetic test indicate southward motion of the Hawaiian mantle plume from 81 to 47 Ma. This result and others indicate that plumes are influenced by mantle flow. Paleomagnetic and age data from volcanic edifices comprising hotspot tracks thus can be used to track past mantle flow. Similarly, the paleointensity data from Leg 197, together with other results, suggest an active lower mantle. By influencing the pattern of heat flux from the core, the mantle can exert some control on the geodynamo. New radiometric dating of the Emperor Seamounts shows that there were several changes in plate relative to hotspot motion, due both to changes in plume advection and Pacific plate motion.

The Hawaiian Islands model for volcano evolution appears to be generally applicable to the volcanoes of the Emperor Seamounts, with adjustment for differences along the chain in lithospheric thickness at the time of construction. Major and trace element compositions of Emperor Seamount lavas conform closely with those at Hawaii. Estimates of size of lava flows, rates of eruption, and timescales of volcano growth are similar along the chain. Because of the change from near-ridge to intraplate environment of hotspot activity, volcanoes at the northern end of the Emperor Seamounts were constructed from higher degrees of melting and shallower depths of melt segregation from the upper mantle, compared with those in the central and southern Emperor Seamounts. Detroit Seamount presents lava compositions that are in many ways MORB-like but are distinguishable in isotopic character (Pb and He) and trace element ratios, which point to an intrinsic plume component present throughout the history of the Hawaiian hotspot.

ACKNOWLEDGMENTS

We thank the editors and reviewers of *Geochemistry, Geophysics, Geosystems* for guiding to publication many of the contributions from Leg 197 scientific results, under the theme "Movement, Dynamics, and Geochemical Evolution of the Hawaiian Hot Spot." This synthesis benefited from reviews by M.F. Coffin and P. Molnar. Our participation in Leg 197 and this synthesis were supported by the U.S. Science Support Program. This research used samples and/or data provided by the Ocean Drilling Program (ODP). ODP is sponsored by the U.S. National Science Foundation and participating countries under management of Joint Oceanographic Institutions (JOI), Inc.

REFERENCES

Anderson, D.L., 2000. The thermal state of the upper mantle: no role for mantle plumes. *Geophys. Res. Lett.,* 27(22):3623–3626. **doi:10.1029/2000GL011533**

Anderson, D.L., 2004. Simple scaling relations in geodynamics: the role of pressure in mantle convection and plume formation. *Chin. Sci. Bull.,* 49:2017–2021.

Anson, G.L., and Kodama, K.P., 1987. Compaction-induced shallowing of the post-depositional remanent magnetization in a synthetic sediment. *Geophys. J. R. Astron. Soc.,* 88:673–692.

Antretter, M., Steinberger, B., Heider, F., and Soffel, H., 2002. Paleolatitudes of the Kerguelen hotspot: new paleomagnetic results and dynamic modeling. *Earth Planet. Sci. Lett.,* 203:635–650. **doi:10.1016/S0012-821X(02)00841-5**

Arason, P., and Levi, S., 1990. Compaction and inclination shallowing in deep-sea sediments from the Pacific Ocean. *J. Geophys. Res.,* 95:4501–4510.

Banerjee, S.K., 2001. Geophysics: when the compass stopped reversing its poles. *Science,* 291(5509):1714–1715. **doi:10.1126/science.291.5509.1714**

Berggren, W.A., Kent, D.V., Swisher, C.C., III, and Aubry, M.-P., 1995. A revised Cenozoic geochronology and chronostratigraphy. *In* Berggren, W.A., Kent, D.V., Aubry, M.-P., and Hardenbol, J. (Eds.), *Geochronology, Time Scales and Global Stratigraphic Correlation*. Spec. Publ.—SEPM (Soc. Sediment. Geol.), 54:129–212.

Besse, J., and Courtillot, V., 2002. Apparent and true polar wander and the geometry of the geomagnetic field over the last 200 Myr. *J. Geophys. Res. [Solid Earth Planets],* 107:11. **doi:10.1029/2000JB000050**

Blichert-Toft, J., Frey, F.A., and Albarede, F., 1999. Hf isotope evidence for pelagic sediments in the source for Hawaiian basalts. *Science,* 285(5429):879–882. **doi:10.1126/science.285.5429.879**

Brock, A., 1971. An experimental study of palaeosecular variation. *Geophys. J. R. Astron. Soc.,* 24:303–317.

Bouska, V., 1993. *Natural Glasses:* New York (Ellis Horwood).

Camps, P., Prevot, M., Daignieres, M., and Machetel, P., 2002. Comment on "stability of the Earth with respect to the spin axis for the last 130 million years" by J.A. Tarduno and A.V. Smirnov [Earth Planet. Sci. Lett, 184 (2001) 549–553]. *Earth Planet. Sci. Lett.,* 198(3–4):529–532. **doi:10.1016/S0012-821X(02)00495-8**

Cande, S.C., and Kent, D.V., 1995. Revised calibration of the geomagnetic polarity timescale for the Late Cretaceous and Cenozoic. *J. Geophys. Res.,* 100(B4):6093–6095. **doi:10.1029/94JB03098**

Cande, S.C., Raymond, C.A., Stock, J., and Haxby, W.F., 1995. Geophysics of the Pitman Fracture Zone and Pacific-Antarctic plate motions during the Cenozoic. *Science,* 270:947–953.

Carvallo, C., Özdemir, Ö., and Dunlop, D.J., 2004a. Paleointensity determinations, paleodirections and magnetic properties of basalts from the Emperor Seamounts. *Geophys. J. Int.,* 156(1):29–38. **doi:10.1111/j.1365-246X.2004.02110.x**

Carvallo, C., Özdemir, Ö., and Dunlop, D.J., 2004b. Palaeointensity determinations, palaeodirections and magnetic properties of basalts from the Emperor Seamounts (vol. 156, pg. 29, 2004). *Geophys. J. Int.,* 158(3):898–898. **doi:10.1111/j.1365-246X.2004.02380.x**

Chen, C.-Y., and Frey, F.A., 1985. Trace element and isotopic geochemistry of lavas from Haleakala Volcano, East Maui, Hawaii: implications for the origin of Hawaiian basalts. *J. Geophys. Res.,* 90:8743–8768.

Christensen, U.R., and Olson, P., 2003. Secular variation in numerical geodynamo models with lateral variations of boundary heat flow. *Phys. Earth Planet. Inter.,* 138(1):39–54. **doi:10.1016/S0031-9201(03)00064-5**

Clague, D.A., and Dalrymple, G.B., 1987. The Hawaiian-Emperor volcanic chain, Part I. Geologic evolution. *In* Decker, R.W., Wright, T.L., and Stauffer, P.H. (Eds.), *Volcanism in Hawaii.* U.S. Geol. Surv. Prof. Pap., 5–73.

Coe, R.S., 1967. The determination of paleointensities of the Earth's magnetic field with emphasis on mechanisms which could cause non-ideal behaviour in Thelliers method. *J. Geomagn. Geoelectr.,* 19:157–179.

Cottrell, R.D., and Tarduno, J.A., 1999. Geomagnetic paleointensity derived from single plagioclase crystals. *Earth Planet. Sci. Lett.,* 169(1–2):1–5. **doi:10.1016/S0012-821X(99)00068-0**

Cottrell, R.D., and Tarduno, J.A., 2000a. In search of high fidelity geomagnetic paleointensities: a comparison of single plagioclase crystal and whole rock Thellier-Thellier analyses. *J. Geophys. Res.,* 105(B10):23579–23594. **doi:10.1029/2000JB900219**

Cottrell, R.D., and Tarduno, J.A., 2000b. Late Cretaceous true polar wander: not so fast. *Science,* 2889(5475):2283a. **doi:10.1126/science.288.5475.2283a**

Cottrell, R.D., and Tarduno, J.A., 2003. A Late Cretaceous pole for the Pacific plate: implications for apparent and true polar wander and the drift of hotspots. *Tectonophysics,* 362(1–4):321–333. **doi:10.1016/S0040-1951(02)00643-1**

Courtillot, V., and Besse, J., 2004. A long-term octupolar component in the geomagnetic field? (0–200 million years b.p.) *In* Channell, J.E.T., Kent, D.V., Lowrie, W., and Meert, J.G., *Timescales of the Paleomagnetic Field*. Geophys. Monogr.,145:59–74.

Courtillot, V., Davaille, A., Besse, J., and Stock, J., 2003. Three distinct types of hotspots in Earth's mantle. *Earth Planet. Sci. Lett.,* 205(3–4):295–308. **doi:10.1016/S0012-821X(02)01048-8**

Cox, A., 1968. Lengths of geomagnetic polarity intervals. *J. Geophys. Res.,* 73:3247–3260.

Cox, A., 1970. Latitude dependence of the angular dispersion of the geomagnetic field. *Geophys. J. R. Astron. Soc.,* 20:253–269.

Dana, J.D., 1849. *The United States Exploring Expedition During the Years 1838–1839, 1840, 1841, 1842* (Vol. 10): *Geology:* Philadelphia (Sherman).

Darwin, C., 1842. *The Structure and Distribution of Coral Reefs (Part 1 of the Geology of the Voyage of the Beagle):* London (Smith, Elder).

DePaolo, D.J., Bryce, J.G., Dodson, A., Schuster, D.L., and Kennedy, B.M., 2001. Isotopic evolution of Mauna Loa and the chemical structure of the Hawaiian plume. *Geochem., Geophys., Geosyst.,* 2(7). **doi:10.1029/2000GC000139**

DiVenere, V., and Kent, D.V., 1999. Are the Pacific and Indo-Atlantic hotspots fixed? Testing the plate circuit through Antarctica. *Earth Planet. Sci. Lett.,* 170(1–2):105–117. **doi:10.1016/S0012-821X(99)00096-5**

Donth, E.-J., 2001. *The Glass Transition: Relaxation Dynamics in Liquids and Disordered Materials:* New York (Springer).

Doubrovine, P.V., and Tarduno, J.A., 2004a. Self-reversed magnetization carried by titanomaghemite in oceanic basalts. *Earth Planet. Sci. Lett.,* 222(3–4):959–969. **doi:10.1016/j.epsl.2004.04.009**

Doubrovine, P.V., and Tarduno, J.A., 2004b. The Late Cretaceous paleolatitude of the Hawaiian hot spot: new paleomagnetic data from Detroit Seamount. *Geochem., Geophys., Geosyst.,* 5:Q11L04. **doi:10.1029/2004GC000745**

Doubrovine, P.V., and Tarduno, J.A., 2005. On the compositional field of self-reversing titanomaghemite: constraints from Deep Sea Drilling Project Site 307. *J. Geophys. Res.,* 110:B11104. **doi:10.1029/2005JB003865**

Duncan, R.A., and Clague, D.A., 1985. Pacific plate motion recorded by linear volcanic chains. *In* Nairn, A.E.M., Stehli, F.G., and Uyeda, S. (Eds.), *The Ocean Basins and Margins* (Vol. 7A): *The Pacific Ocean:* New York (Plenum), 89–121.

Duncan, R.A., and Keller, R.A., 2004. Radiometric ages for basement rocks from the Emperor Seamounts, ODP Leg 197. *Geochem., Geophys., Geosyst.,* 5(8):Q08L03. **doi:10.1029/2004GC000704**

Dunlop, D.J., and Özdemir, Ö., 1997. *Rock Magnetism: Fundamentals and Frontiers:* Cambridge (Cambridge Univ. Press).

Dunlop, D.J., Zhang, B., and Ozdemir, O., 2005. Linear and nonlinear Thellier paleointensity behavior of natural minerals. *J. Geophys. Res.,* 110:B01103. **doi:10.1029/2004JB003095**

Fisher, R.A., 1953. Dispersion on a sphere. *Proc. R. Soc. London, Ser. A,* 217:295–305.

Foulger, G.R., and Natland, J.H., 2003. Geology: is "hotspot" volcanism a consequence of plate tectonics? *Science,* 300(5621):921–922. **doi:10.1126/science.1083376**

Frey, F.A., Huang, S., Blichert-Toft, J., Regelous, M., and Boyet, M., 2005. Origin of depleted components in basalt related to the Hawaiian hot spot: evidence from isotopic and incompatible element ratios. *Geochem., Geophys., Geosyst.,* 6(2):Q02L07. **doi:10.1029/2004GC000757**

Gaffney, A.M., Nelson, B.K., and Blichert-Toft, J., 2005. Melting in the Hawaiian plume at 1–2 Ma as recorded at Maui Nui: the role of eclogite, peridotite and source mixing. *Geochem., Geophys., Geosyst.,* 6(10):Q10L11. **doi:10.1029/2005GC000927**

Gallet, Y., and Hulot, G., 1997. Stationary and nonstationary behaviour within the geomagnetic polarity time scale. *Geophys. Res. Lett.,* 24(15):1875–1878. **doi:10.1029/97GL01819**

Glatzmaier, G.A., Coe, R.S., Hongre, L., and Roberts, P.H., 1999. The role of the Earth's mantle in controlling the frequency of geomagnetic reversals. *Nature (London, U. K.),* 401(6756):885–890. **doi:10.1038/44776**

Goguitchaichvili, A., Alva-Vaeldivia, L.M., Rosas-Elguera, J., Urrutia-Fucugachi, J., and Sole, J., 2004. Absolute geomagnetic paleointensity after the Cretaceous Normal Superchron and just prior to the Cretaceous–Tertiary transition. *J. Geophys. Res.,* 109:B01105. **doi:10.1029/2003JB002477**

Goldreich, P., and Toomre, A., 1969. Some remarks on polar wandering. *J. Geophys. Res.,* 74:2555–2567.

Gradstein, F.M., Ogg, J.G., and Smith, A. (Eds.), 2004. *A Geologic Time Scale 2004:* Cambridge (Cambridge Univ. Press).

Gromme, S., Mankinen, E.A., Marshall, M., and Coe, R.S., 1979. Geomagnetic paleointensities by the Thelliers' method from submarine pillow basalts: effects of seafloor weathering. *J. Geophys. Res.,* 84:3553–3575.

Harada, Y., and Hamano, Y., 2000. Recent progress on the plate motion relative to hotspots. *In* Richards, M.A., Gordon, R.G., and Van der Hilst, R.D. (Eds.), *The History and Dynamics of Global Plate Motions.* Geophys. Monogr., 121:327–338.

Hauri, E.H., 1996. Major-element variability in the Hawaiian mantle plume. *Nature (London, U. K.),* 382(6590):415–419. **doi:10.1038/382415a0**

Heller, R., Merrill, R.T., and McFadden, P.L., 2002. The variation of intensity of Earth's magnetic field with time. *Phys. Earth Planet. Inter.,* 131(3–4):237–249. **doi:10.1016/S0031-9201(02)00038-9**

Huang, S., Regelous, M., Thordarson, T., and Frey, F.A., 2005. Petrogenesis of lavas from Detroit Seamount: geochemical differences between Emperor chain and Hawaiian volcanoes. *Geochem., Geophys., Geosyst.,* 6:Q01L06. **doi:10.1029/2004GC000756**

Hulot, G., and Gallet, Y., 2003. Do superchrons occur without paleomagnetic warning? *Earth Planet. Sci. Lett.,* 210(1–2):191–201. **doi:10.1016/S0012-821X(03)00130-4**

Kerr, B.C., Scholl, D.W., and Klemperer, S.L., 2005. Seismic stratigraphy of Detroit Seamount, Hawaiian-Emperor Seamount chain: post-hotspot shield-building volcanism and deposition of the Meiji drift. *Geochem., Geophys., Geosyst.,* 6:Q07L10. **doi:10.1029/2004GC000705**

Keller, R.A., Fisk, M.R., and White, W.M., 2000. Isotopic evidence for Late Cretaceous plume-ridge interaction at the Hawaiian hotspot. *Nature (London, U. K.),* 405(6787):673–676. **doi:10.1038/35015057**

Keller, R.A., Graham, D.W., Farley, K.A., Duncan, R.A., and Lupton, J.E., 2004. Cretaceous-to-recent record of elevated $^{3}He/^{4}He$ along the Hawaiian-Emperor volcanic chain. *Geochem., Geophys., Geosyst.,* 5:Q12L05. **doi:10.1029/2004GC000739**

Kono, M., 1980. Paleomagnetism of DSDP Leg 55 basalts and implications for the tectonics of the Pacific plate. *In* Jackson, E.D., Koizumi, I., et al., *Init. Repts. DSDP,* 55: Washington (U.S. Govt. Printing Office), 737–752.

Koppers, A.A.P., Duncan, R.A., and Steinberger, B., 2004. Implications of a nonlinear $^{40}Ar/^{39}Ar$ age progression along the Louisville seamount trail for models of fixed and moving hot spots. *Geochem., Geophys., Geosyst.,* 5:Q06L02. **doi:10.1029/2003GC000671**

Koppers, A.A.P., and Staudigel, H., 2005. Asynchronous bends in Pacific seamount trails: a case for extensional volcanism? *Science,* 307(5711):904–907. **doi:10.1126/science.1107260**

Koppers, A.A.P., Staudigel, H., and Wijbrans, J.R., 2000. Dating crystalline groundmass separates of altered Cretaceous seamount basalts by the $^{40}Ar/^{39}Ar$ incremental heating technique. *Chem. Geol.,* 166(1–2):139–158. **doi:10.1016/S0009-2541(99)00188-6**

Kroenke, L.W., Wessel, P., and Sterling, A.I., 2004. Motion of the Ontong Java Plateau in the hotspot frame of reference: 122 Ma–present. *In* Fitton, J.G., Mahoney, J.J., Wallace, P.J., and Saunders, A.D. (Eds.), *Origin and Evolution of the Ontong Java Plateau.* Geol. Soc. Spec. Publ., 229:9–20.

Larson, R.L., and Olson, P., 1991. Mantle plumes control magnetic reversal frequency. *Earth Planet. Sci. Lett.,* 107(3–4):437–447. **doi:10.1016/0012-821X(91)90091-U**

Lassiter, J.C., and Hauri, E.H., 1998. Osmium-isotope variations in Hawaiian lavas: evidence for recycled oceanic lithosphere in the Hawaiian plume. *Earth Planet. Sci. Lett.,* 164(3–4):483–496. **doi:10.1016/S0012-821X(98)00240-4**

Lowrie, W., and Kent, D.V., 2004. Geomagnetic polarity timescales and reversal frequency regimes *In* Channell, J.E.T., Kent. D.V., Lowrie, W., and Meert, J.G., *Timescales of the Paleomagnetic Field.* Geophys. Monogr., 145:117–129.

McDougall, I., 1964. Potassium-argon ages from lavas of the Hawaiian Islands. *Geol. Soc. Am. Bull.,* 75:107–128.

McElhinny, M.W., and Larson, R.L., 2003. Jurassic dipole low defined from land and sea data. *Eos, Trans. Am. Geophys. Union,* 84:362–366.

McFadden, P.L., Merrill, R.T., McElhinny, M.W., and Lee, S., 1991. Reversals of the Earth's magnetic field and temporal variations of the dynamo families. *J. Geophys. Res.,* 96:3923–3933. **doi:10.1029/90JB02275**

McFadden, P.L., and Reid, A.B., 1982. Analysis of paleomagnetic inclination data. *Geophys. J. R. Astron. Soc.,* 69:307–319.

Molnar, P., and Atwater, T., 1973. Relative motion of hot spots in the mantle. *Nature (London, U. K.),* 246(5431):288–291. **doi:10.1038/246288a0**

Molnar, P., and Stock, J., 1987. Relative motions of hotspots in the Pacific, Atlantic, and Indian Oceans since Late Cretaceous time. *Nature (London, U. K.),* 327(6123):587–591. **doi:10.1038/327587a0**

Montelli, R., Nolet, G., Dahlen, F.A., Masters, G., Engdahl, E.R., and Hung, S.H., 2004. Finite-frequency tomography reveals a variety of plumes in the mantle. *Science,* 303(5656):338–343. **doi:10.1126/science.1092485**

Moore, T.C., Jr., Backman, J., Raffi, I., Nigrini, C., Sanfilippo, A., Pälike, H., and Lyle, M., 2004. Paleogene tropical Pacific: clues to circulation, productivity, and plate motion. *Paleoceanography,* 19(3):PA3013. **doi:10.1029/2003PA000998**

Morgan, W.J., 1971. Convection plumes in the lower mantle. *Nature (London, U. K.),* 230(5288):42–43. **doi:10.1038/230042a0**

Mueller, R.D., Roest, W.R., Royer, J.-Y., Gahagan, L.M., and Sclater, J.G., 1997. Digital isochrons of the world's ocean floor. *J. Geophys. Res.,* 102(b2):3211–3214. **doi:10.1029/96JB01781**

Norton, I.O., 1995. Plate motions in the North Pacific: the 43 Ma nonevent. *Tectonics,* 14(5):1080–1094. **doi:10.1029/95TC01256**

Olson, P., and Christensen, U.R., 2002. The time-averaged magnetic field in numerical dynamos with non-uniform boundary heat flow. *Geophys. J. Int.,* 151(3):809–823. **doi:10.1046/j.1365-246X.2002.01818.x**

Opdyke, N.D., and Channell, J.E.T., 1996. *Magnetic Stratigraphy:* International Geophys. Ser., vol. 64. New York (Academic Press).

O'Reilly, W., and Banerjee, S.K., 1966. Oxidation of titanomagnetites and self-reversal. *Nature (London, U. K.),* 211:26–28.

Pares, J.M., and Moore, T.C., 2005. New evidence for Hawaiian hotspot plume motion since the Eocene. *Earth Planet. Sci. Lett.,* 237(3–4):951–959. **doi:10.1016/j.epsl.2005.06.012**

Pick, T., and Tauxe, L., 1993. Geomagnetic paleointensities during the Cretaceous normal superchron measured using submarine basaltic glass. *Nature (London, U. K.),* 366(6452):238–242. **doi:10.1038/366238a0**

Pike, C.R., Roberts, A.P., and Verosub, K.L., 1999. Characterizing interactions in fine magnetic particles systems using first order reversal curves. *J. Appl. Phys.,* 85(9):6660–6667. **doi:10.1063/1.370176**

Prevot, M., Mattern, E., Camps, P., and Daignieres, M., 2000. Evidence for a 20° tilting of the Earth's rotation axis 110 million years ago. *Earth Planet. Sci. Lett.,* 179(3–4):517–528. **doi:10.1016/S0012-821X(00)00129-1**

Raymond, C.A., Stock, J.M., and Cande, S.C., 2000. Fast Paleogene motion of the Pacific hotspots from revised global plate circuit constraints. *In* Richards, M.A., Gordon, R.G., and van der Hilst, R.D. (Eds.), *The History and Dynamics of Global Plate Motions*. Geophys. Monogr., 121:359–375.

Ren, Z.-Y., Ingle, S., Takahashi, E., Hirano, N., and Hirata, T., 2005. The chemical structure of the Hawaiian mantle plume. *Nature (London, U. K.),* 436(7052):837–840. **doi:10.1038/nature03907**

Riisager, P., Hall, S., Antretter, M., and Zhao, X., 2003. Paleomagnetic paleolatitude of Early Cretaceous Ontong Java Plateau basalts: implications for Pacific Apparent and True Polar Wander. *Earth Planet. Sci. Lett.,* 208(3–4):235–252. **doi:10.1016/S0012-821X(03)00046-3**

Riisager P., Riisager, J, Zhao, X., and Coe, R.S., 2003. Cretaceous geomagnetic paleointensities: Thellier experiments on pillow lavas and submarine basaltic glass from the Ontong Java Plateau. *Geochem., Geophys., Geosyst.,* 4(12):8803. **doi:10.1029/2003GC000611**

Roberts, A.P., Pike, C.R., and Verosub, K.L., 2000. FORC diagrams: a new tool for characterizing the magnetic properties of natural samples. *J. Geophys. Res.,* 105(B12):28461–28475. **doi:10.1029/2000JB900326**

Roberts, P.H., and Glatzmaier, G.A., 2000. Geodynamo theory and simulations. *Rev. Mod. Phys.,* 72(4):1081–1123. **doi:10.1103/RevModPhys.72.1081**

Sager, W.W., 2002. Basalt core paleomagnetic data from Ocean Drilling Program Site 883 on Detroit Seamount, northern Emperor Seamount chain, and implications for the paleolatitude of the Hawaiian hotspot. *Earth Planet. Sci. Lett.,* 199(3–4):347–358. **doi:10.1016/S0012-821X(02)00590-3**

Selkin, P.A., and Tauxe, L., 2000. Long-term variations in palaeointensity. *Philos. Trans. R. Soc. London, Ser. A,* 358:1065–1088. **doi:10.1098/rsta.2000.0574**

Shafer, J.T., Neal, C.R., and Regelous, M., 2005. Petrogenesis of Hawaiian postshield lavas: evidence from Nintoku Seamount, Emperor Seamount chain. *Geochem., Geophys., Geosyst.,* 6:Q05L09. **doi:10.1029/2004GC000875**

Sharp, W.D., and Clague, D.A., 2002. An older slower Hawaii–Emperor bend. *Eos, Trans. Am. Geophys. Union,* 83:F1282.

Sleep, N.H., 2003. Mantle plumes. *Astron. Geophys.,* 44(1):1.11–1.13. **doi:10.1046/j.1468-4004.2003.44111.x**

Smirnov, A.V., and Tarduno, J.A., 2003. Magnetic hysteresis monitoring of Cretaceous submarine basaltic glass during Thellier paleointensity experiments: evidence for alteration and attendant low field bias. *Earth Planet. Sci. Lett.,* 206(3–4):571–585. **doi:10.1016/S0012-821X(02)01123-8**

Smirnov, A.V., and Tarduno, J.A., 2005. Thermochemical remanent magnetization in Precambrian rocks: are we sure the geomagnetic field was weak? *J. Geophys. Res.,* 110:B06103. **doi:10.1029/2004JB003445**

Smirnov, A.V., Tarduno, J.A., and Pisakin, B.N., 2003. Paleointensity of the early geodynamo (2.45 Ga) as recorded in Karelia: a single-crystal approach. *Geology,* 31(5):415–418. **doi:10.1130/0091-7613(2003)031<0415:POTEGG>2.0.CO;2**

Steinberger, B., 2000. Plumes in a convecting mantle: models and observations for individual hotspots. *J. Geophys. Res.,* 105(B5):11127–11152. **doi:10.1029/1999JB900398**

Steinberger, B., and O'Connell, R.J., 1998. Advection of plumes in mantle flow: implications for hotspot motion, mantle viscosity and plume distribution. *Geophys. J. Int.,* 132(2):412–434. **doi:10.1046/j.1365-246x.1998.00447.x**

Steinberger, B., Sutherland, R., and O'Connell, R.J., 2004. Prediction of Emperor–Hawaii Seamount locations from a revised model of global plate motion and mantle flow. *Nature (London, U. K.),* 430(6996):167–173. **doi:10.1038/nature02660**

Tarduno, J.A., 1990. Absolute inclination values from deep sea sediments: a reexamination of the Cretaceous Pacific record. *Geophys. Res. Lett.,* 17:101–104.

Tarduno, J.A., and Cottrell, R.D., 1997. Paleomagnetic evidence for motion of the Hawaiian hotspot during formation of the Emperor Seamounts. *Earth Planet. Sci. Lett.,* 153(3–4):171–180. **doi:10.1016/S0012-821X(97)00169-6**

Tarduno, J.A., and Cottrell, R.D., 2005. Dipole strength and variation of the time-averaged reversing and nonreversing geodynamo based on Thellier analyses of single plagioclase crystals. *J. Geophys. Res.,* 110:B11101. **doi:10.1029/2005JB003970**

Tarduno, J.A., Cottrell, R.D., and Smirnov, A.V., 2001. High geomagnetic field intensity during the mid-Cretaceous from Thellier analyses of single plagioclase crystals. *Science,* 291(5509):1179–1183. **doi:10.1126/science.1057519**

Tarduno, J.A., Cottrell, R.D., and Smirnov, A.V., 2002. The Cretaceous superchron geodynamo: observations near the tangent cylinder. *Proc. Nat. Acad. Sci. U. S. A.,* 99(22):14020–14025. **doi:10.1073/pnas.222373499**

Tarduno, J.A., Duncan, R.A., Scholl, D.W., Cottrell, R.D., Steinberger, B., Thordarson, T., Kerr, B.C., Neal, C.R., Frey, F.A., Torii, M., and Carvallo, C., 2003. The Emperor Seamounts: southward motion of the Hawaiian hotspot plume in Earth's mantle. *Science,* 301:1064–1069. **doi:10.1126/science.1086442**

Tarduno, J.A., Duncan, R.A., Scholl, D.W., et al., 2002. *Proc. ODP, Init. Repts.,* 197 [CD-ROM]. Available from: Ocean Drilling Program, Texas A&M University, College Station TX 77845-9547, USA. [**HTML**]

Tarduno, J.A., and Gee, J., 1995. Large scale motion between Pacific and Atlantic hotspots. *Nature (London, U. K.),* 378(6556):477–480. **doi:10.1038/378477a0**

Tarduno, J.A., and Smirnov, A.V., 2001. Stability of the Earth with respect to the spin axis for the last 130 million years. *Earth Planet. Sci. Lett.,* 184:549–553. **doi:10.1016/S0012-821X(00)00348-4**

Tarduno, J.A., and Smirnov, A.V., 2002. Response to comment on "stability of the Earth with respect to the spin axis for the last 130 million years" by P. Camps, M. Prevot, M. Daignieres, and P. Machetel. *Earth Planet. Sci. Lett.,* 198(3–4):533–539. **doi:10.1016/S0012-821X(02)00496-X**

Tarduno, J.A., and Smirnov, A.V., 2004. The paradox of low field values and the long-term history of the geodynamo. *In* Channell, J.E.T., Kent, D.V., Lowrie, W., and Meert, J.G., *Timescale of the Internal Geomagnetic Field.* Geophys. Monogr., 145:75–84.

Tauxe, L., and Staudigel, H., 2004. Strength of the geomagnetic field in the Cretaceous Normal Superchron: new data from submarine basaltic glass of the Troodos ophiolite. *Geochem., Geophys., Geosyst.,* 5:Q02H06. **doi:10.1029/2003GC000635**

Thellier, E., and Thellier, O., 1959. Sur l'intensité du champ magnétique terreste dans le passé historique et geologique. *Ann. Geophys.,* 15:285–375.

Torsvik, T.H., Van der Voo, R., and Redfield, T.F., 2002. Relative hotspot motions versus true polar wander. *Earth Planet Sci. Lett.,* 202(2):185–200. **doi:10.1016/S0012-821X(02)00807-5**

Van der Voo, R., and Torsvik, T.H., 2001. Evidence for late Paleozoic and Mesozoic non-dipole fields provides an explanation for the Pangea reconstruction problems. *Earth Planet. Sci. Lett.,* 187(1–2):71–81. **doi:10.1016/S0012-821X(01)00285-0**

Verhoogen, J., 1956. Ionic ordering and self-reversal in impure magnetites *J. Geophys. Res.,* 61:201–209.

Verhoogen, J., 1962. Oxidation of iron-titanium oxides in igneous rocks. *J. Geol.,* 70:168–181.

Van Ark, E., and Lin, J., 2004. Time variation in igneous volume flux of the Hawaii–Emperor hotspot seamount chain. *J. Geophys. Res.,* 109:B11401. **doi:10.1029/2003JB002949**

Watts, A.B., Weissel, J.K., Duncan, R.A., and Larson, R.L., 1988. Origin of the Louisville Ridge and its relationship to the Eltanin Fracture Zone. *J. Geophys. Res.,* 93:3051–3077.

Wessel, P., and Kroenke, L.W., 1997. A geometric technique for relocating hotspots and refining absolute plate motions. *Nature (London, U. K.),* 387(6631):365–369. **doi:10.1038/387365a0**

Wessel, P., and Kroenke, L.W., 1998. The geometric relationship between hotspots and seamounts: implications for Pacific hotspots. *Earth Planet. Sci. Lett.,* 158(1–2):1–18. **doi:10.1016/S0012-821X(98)00043-0**

Wessel, P., and Lyons, S., 1997. Distribution of large Pacific seamounts from Geosat/ERS-1: implications for the history of intraplate volcanism. *J. Geophys. Res.,* 102(B10):22459–22476. **doi:10.1029/97JB01588**

Wilson, J.T., 1963. A possible origin of the Hawaiian Islands. *Can. J. Phys.,* 41:863–870.

Figure F1. ODP Leg 197 sites in the Emperor Seamounts with ages of selected sites (Ma) and seafloor magnetic isochrons (Mueller et al., 1997). Inset shows volcanic centers in the Hawaiian Islands with Loa and Kea compositional trends (modified from Tarduno et al., 2003).

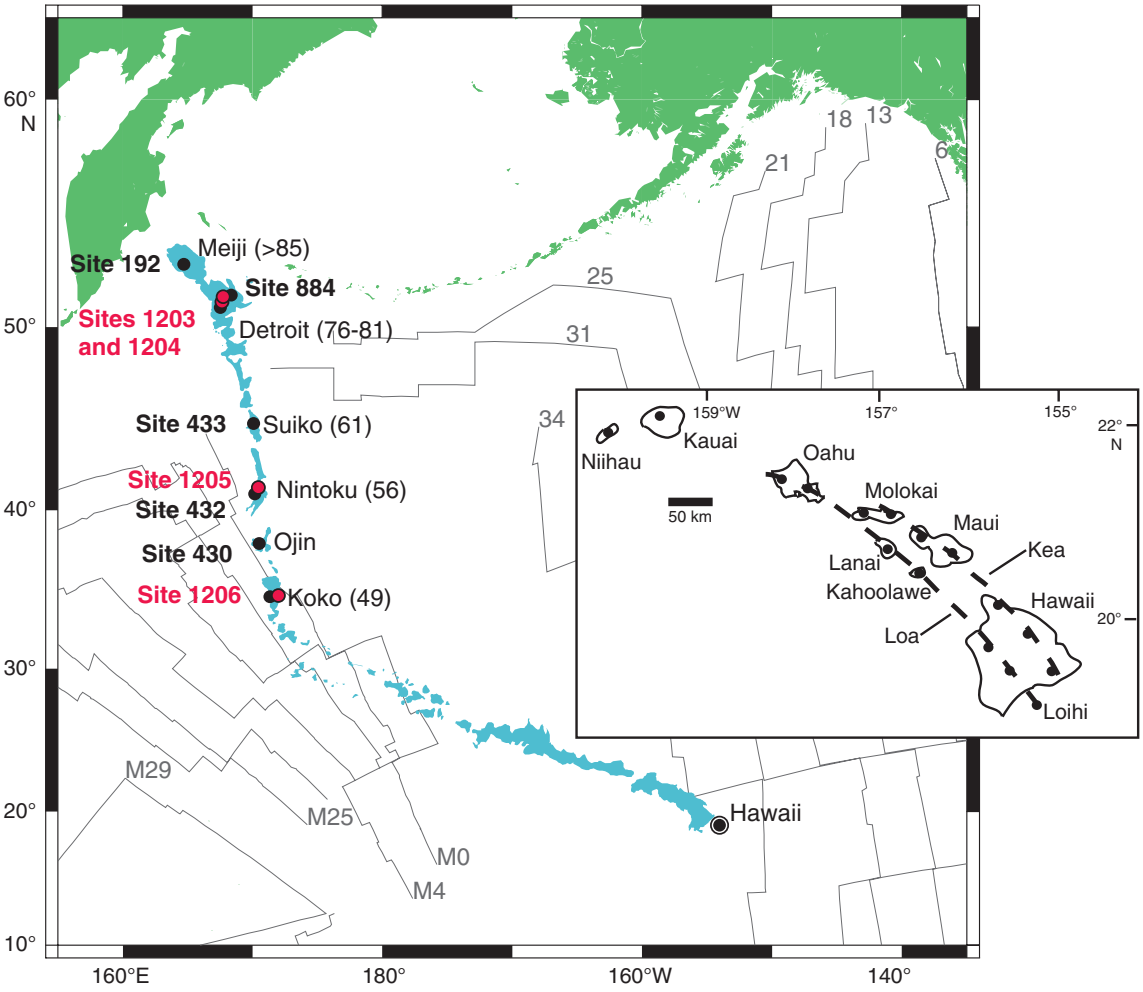

Figure F2. Paleomagnetic inclination groups for Sites (**A**) 1206, (**B**) 1205, (**C**) 1204, and (**D**) 1203 based on thermal demagnetization data (blue) shown compared with a synthetic Fisher distribution (magenta) that has the same mean as the experimental data and a dispersion predicted by global lava data (McFadden et al., 1991). Latitude of Hawaii, mean basalt inclination value (thermal demagnetization) for Hole 1204A (C, green), mean sediment inclination value (thermal demagnetization) for Site 1203 (D), and mean inclination value from ODP Site 883 basalts (Doubrovine and Tarduno, 2004b) are also shown (after Tarduno et al., 2003).

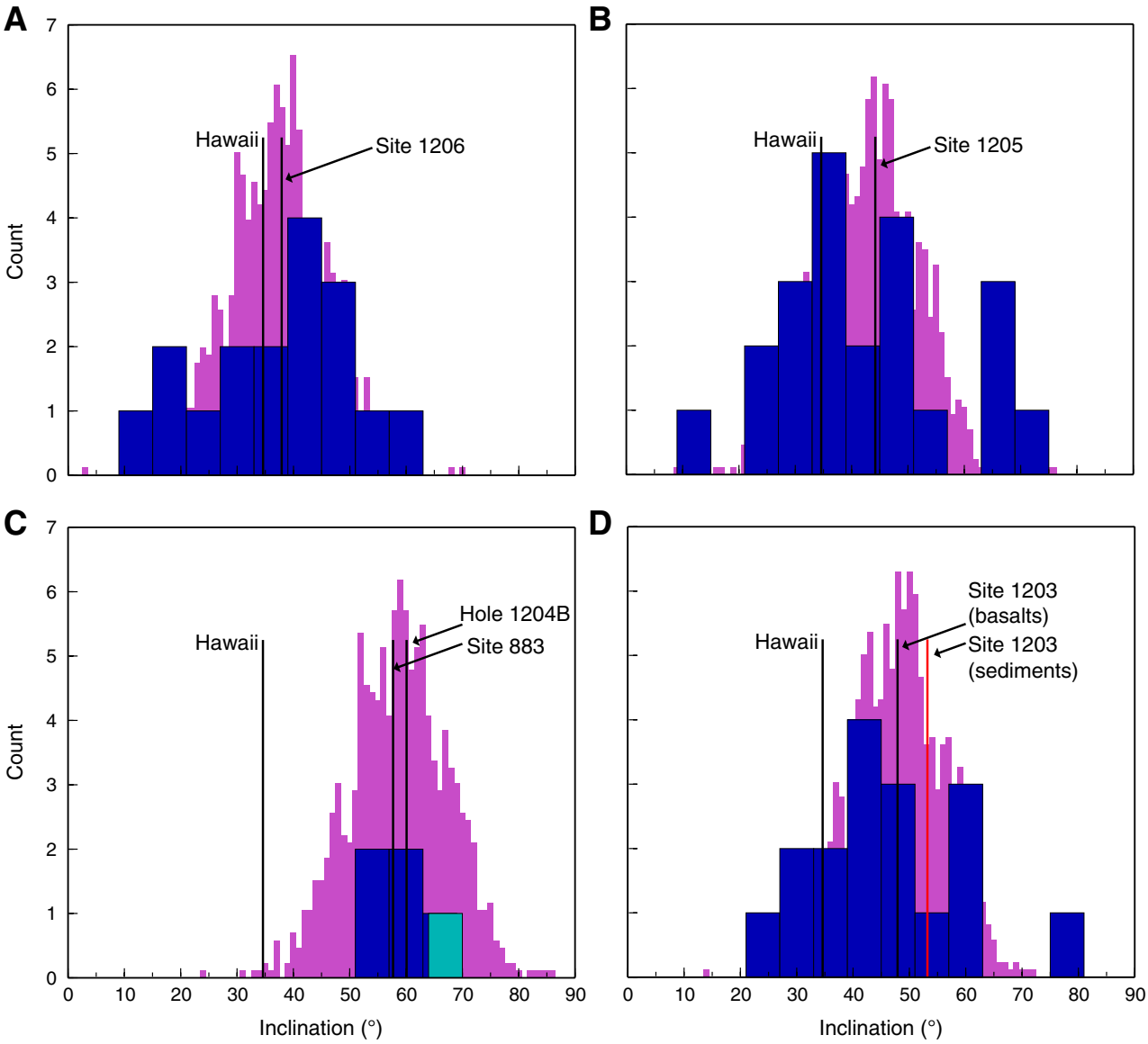

Figure F3. A. Paleolatitude data from Leg 197 sites (1206, Koko Seamount; 1205, Nintoku Seamount; and 1204B and 1203, Detroit Seamount), ODP Site 884 (Detroit Seamount; Tarduno and Cottrell, 1997), ODP Site 883 (Doubrovine and Tarduno, 2004b), and DSDP Site 433 (Suiko Seamount; Kono, 1980). Red = results of thermal demagnetization; blue = results of alternating-field (AF) demagnetization. Result from Site 433 is based on AF and thermal data. Magenta = magnetization carried by hematite from weathered basalt from Site 1206. **B.** Average paleolatitude value for Detroit Seamount (square) based on inclination groups derived from basalts of Sites 884 and 1203 and Hole 1204B (see text) plotted with select paleolatitude values from other seamounts (see A). Also shown is a least-squares fit to the data (red) and several paleolatitude trajectories representing combinations of plate and hotspot motion. Geomagnetic polarity timescale is from Cande and Kent (1995) (after Tarduno et al., 2003).

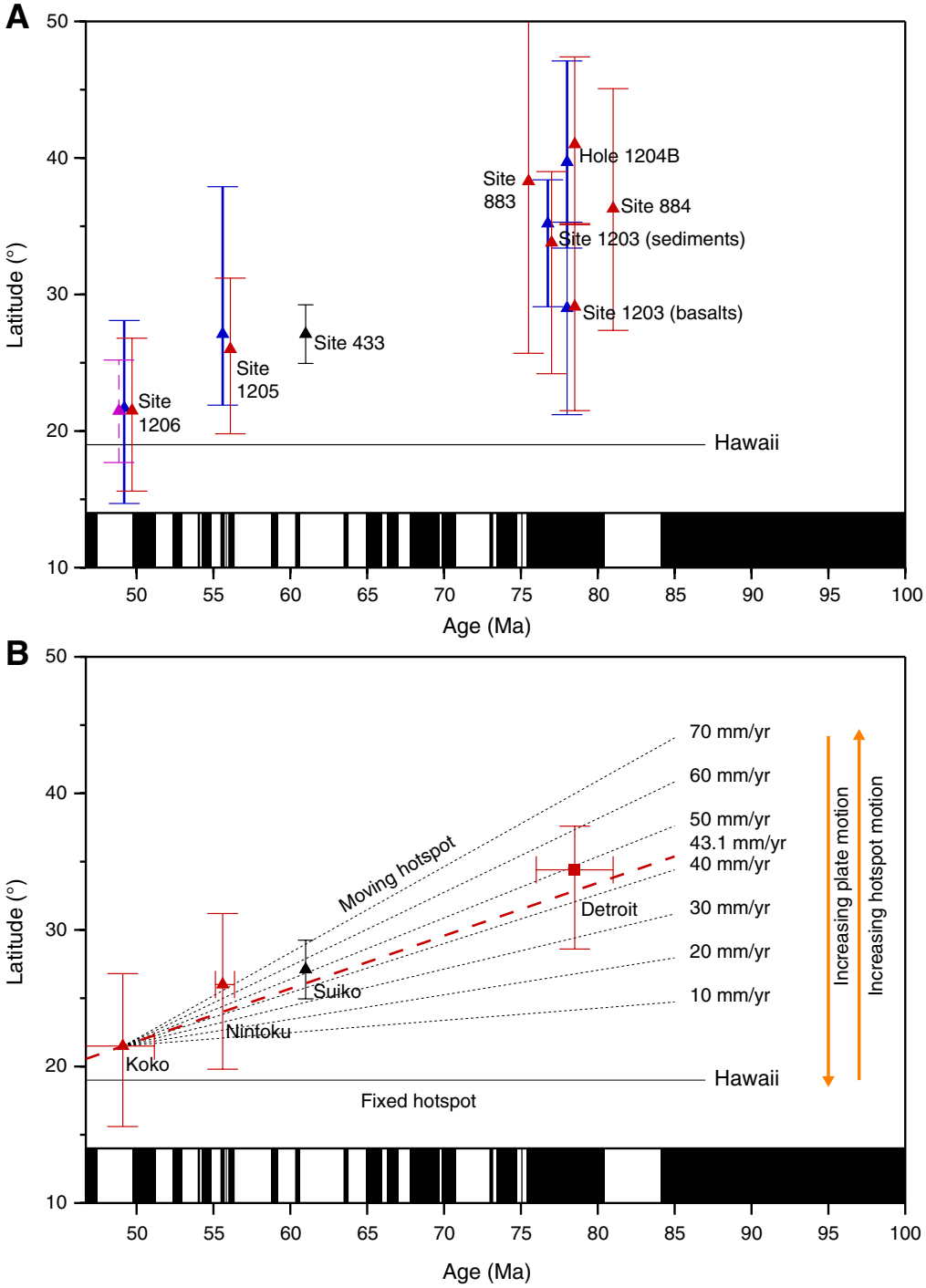

Figure F4. Comparison of geodynamic model results (Steinberger, 2000) and Leg 197 paleomagnetic results. **A.** Computed Hawaiian hotspot motion for moving source model (colored line) and tracks for fixed-source model (solid line; plume initiation at 160 Ma) and moving source model (dashed line; plume initiation at 170 Ma). Tick marks are 10-m.y. increments. **B.** Computed changes of hotspot latitude for fixed-source (solid red lines) for plume initiation ages of 150, 160, and 170 Ma (upper to lower). Moving source model results (dashed lines) are shown for plume initiation at 180, 170, and 160 Ma (upper to lower). Paleolatitude means for Koko, Nintoku, Suiko, and Detroit Seamounts (Model B, see text) are also shown. * = revised age for Suiko Seamount (Sharp and Clague, 2002) (after Tarduno et al., 2003).

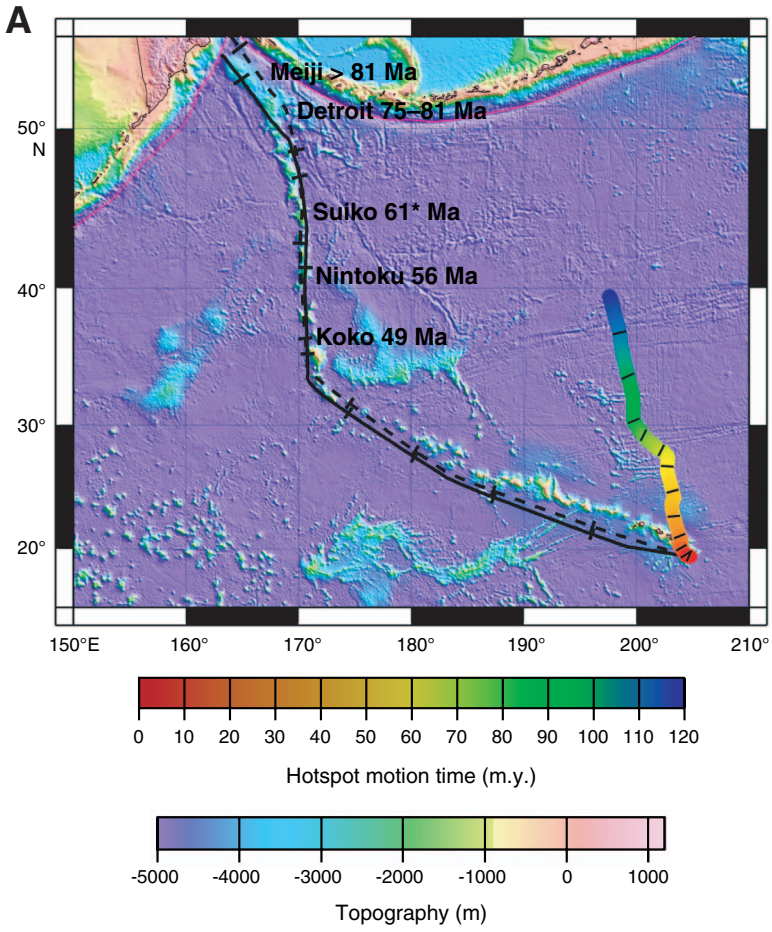

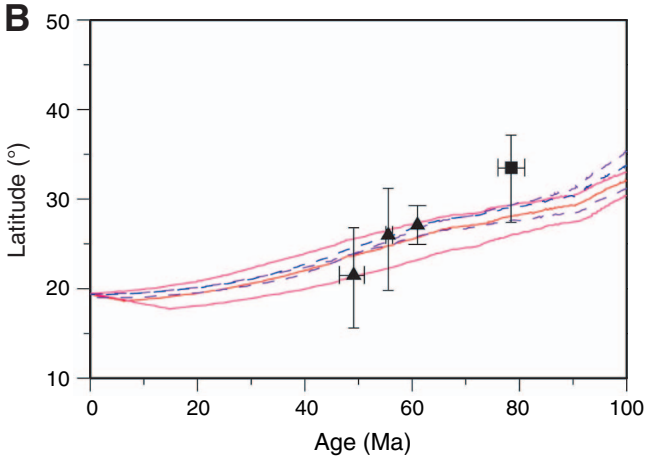

Figure F5. Example of paleointensity data using submarine basaltic glass from Site 1203 (from Smirnov and Tarduno, 2003). **A.** Thermal demagnetization of natural remanent magnetization (NRM). **B.** Acquisition of thermal remanent magnetization (TRM). **C.** Orthogonal vector plot of field-off steps (sample is unoriented). Open squares = vertical projection of NRM, solid circles = horizontal projection. **D.** NRM/TRM plot (circles). Squares = partial TRM experimental checks. **E.** Magnetic hysteresis parameters as a function of temperature on a monitor sample. The total saturation magnetization (*M*s total) is shown before slope correction together with the paramagnetic contribution. The change in these curves denotes experimentally-induced alteration.

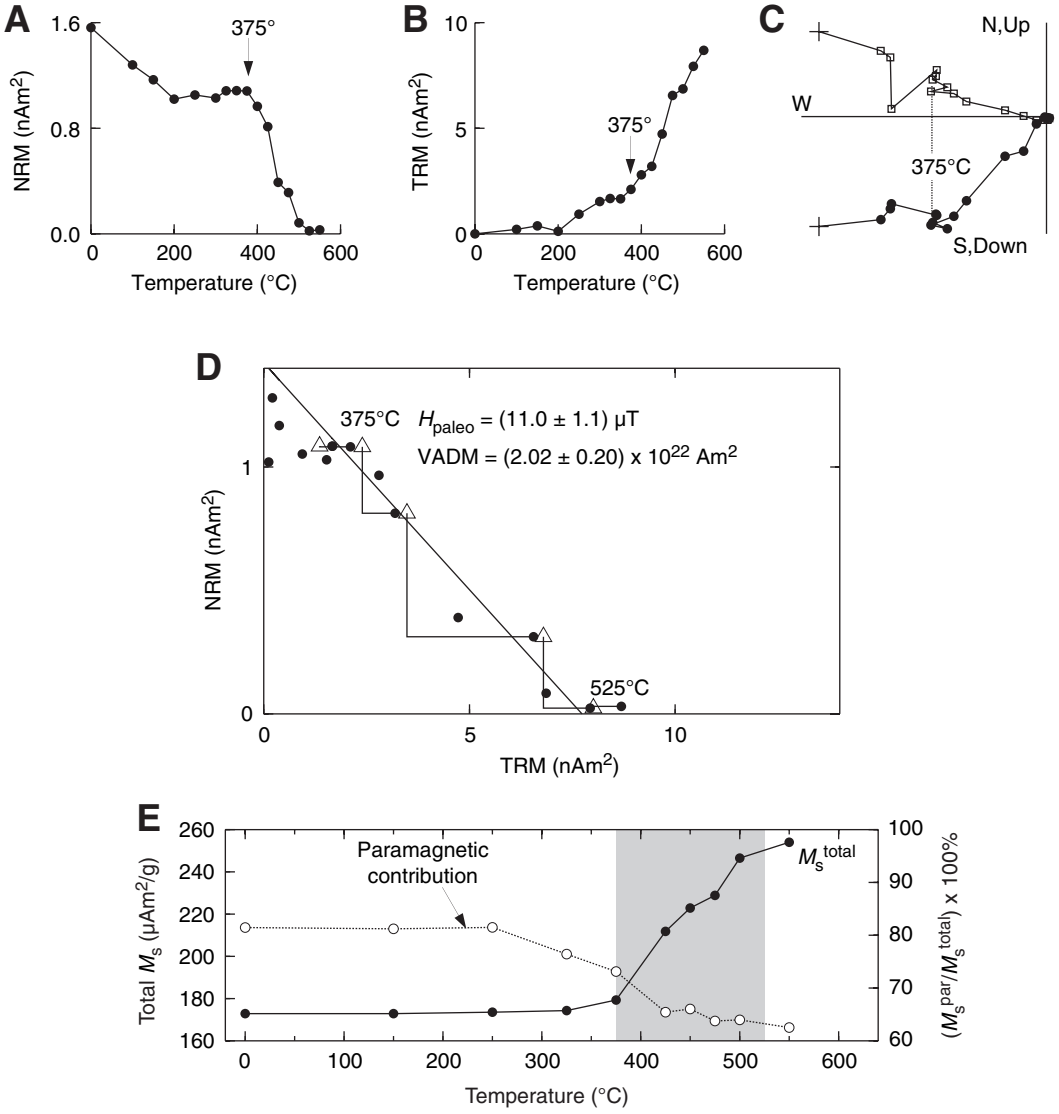

Figure F6. First-order reversal curve (FORC) (Pike et al., 1999; Roberts et al., 2000) diagrams for Nintoku Seamount Site 1205. Diagrams are based on 50 curves and use a smoothing factor of 5 (after Tarduno and Cottrell, 2005).

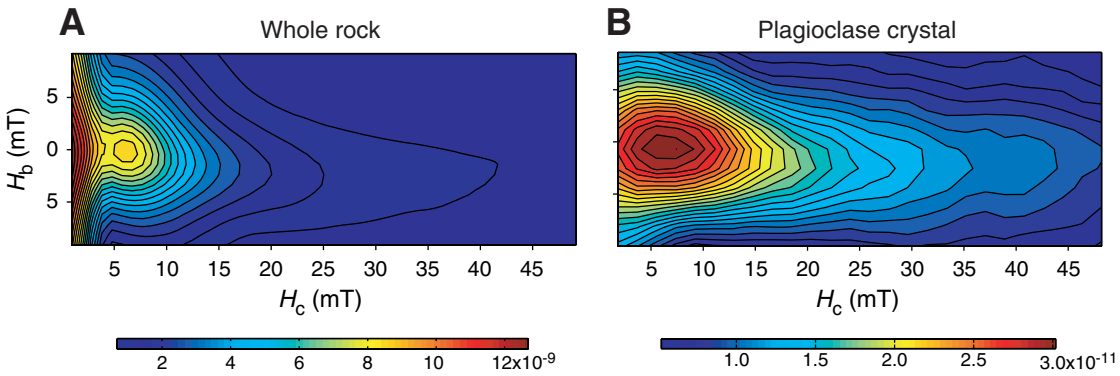

Figure F7. Typical paleointensity results from plagioclase crystals from Nintoku Seamount Site 1205. Experimental checks (see discussion in Tarduno and Cottrell, 2005) are shown by triangles. Labeled points are temperature (degrees C) representing the range used to determine paleointensity. Also shown is summary of paleointensity data grouped in cooling units meeting experimental reliability criteria.

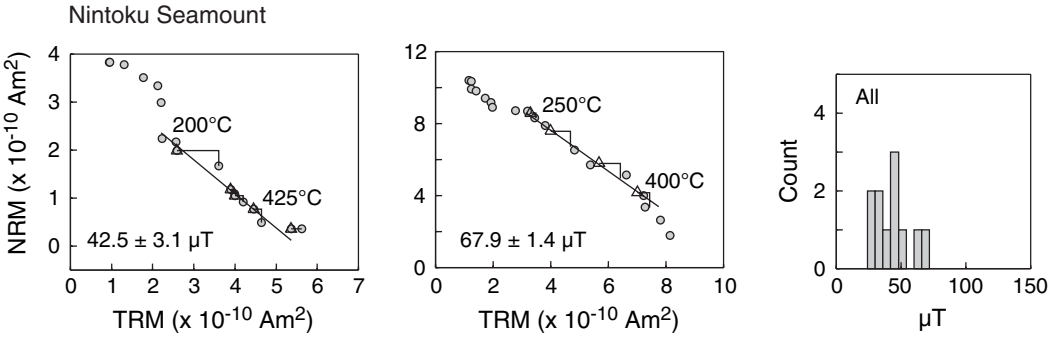

Figure F8. Thellier results from analyses of plagioclase crystals (after Tarduno and Cottrell, 2005) and paleointensity results from whole-rock lava samples from Carvallo et al. (2004a, 2004b) (square). Inset: expanded 165- to 155-Ma reversal chronology (Opdyke and Channell, 1996; Gradstein et al., 2004). Small circles = virtual dipole moments (VDM, cooling unit means of multiple single plagioclase crystal results) from Tarduno et al. (2001, 2002) and Tarduno and Cottrell (2005) (blue = Site 1205 results). Large symbols = averages of the VDMs, comprising paleomagnetic dipole moments, with 1σ uncertainties. Dashed line = variation of paleomagnetic dipole moment standard variations consistent with the available data from single plagioclase crystals. Reversal rate curve is based on a 10-m.y. sliding window. Also shown is division of the reversal chronology into stationary and nonstationary intervals (A, B, C) from Gallet and Hulot (1997). Geomagnetic polarity timescale is from Cande and Kent (1995) and Gradstein et al. (2004).

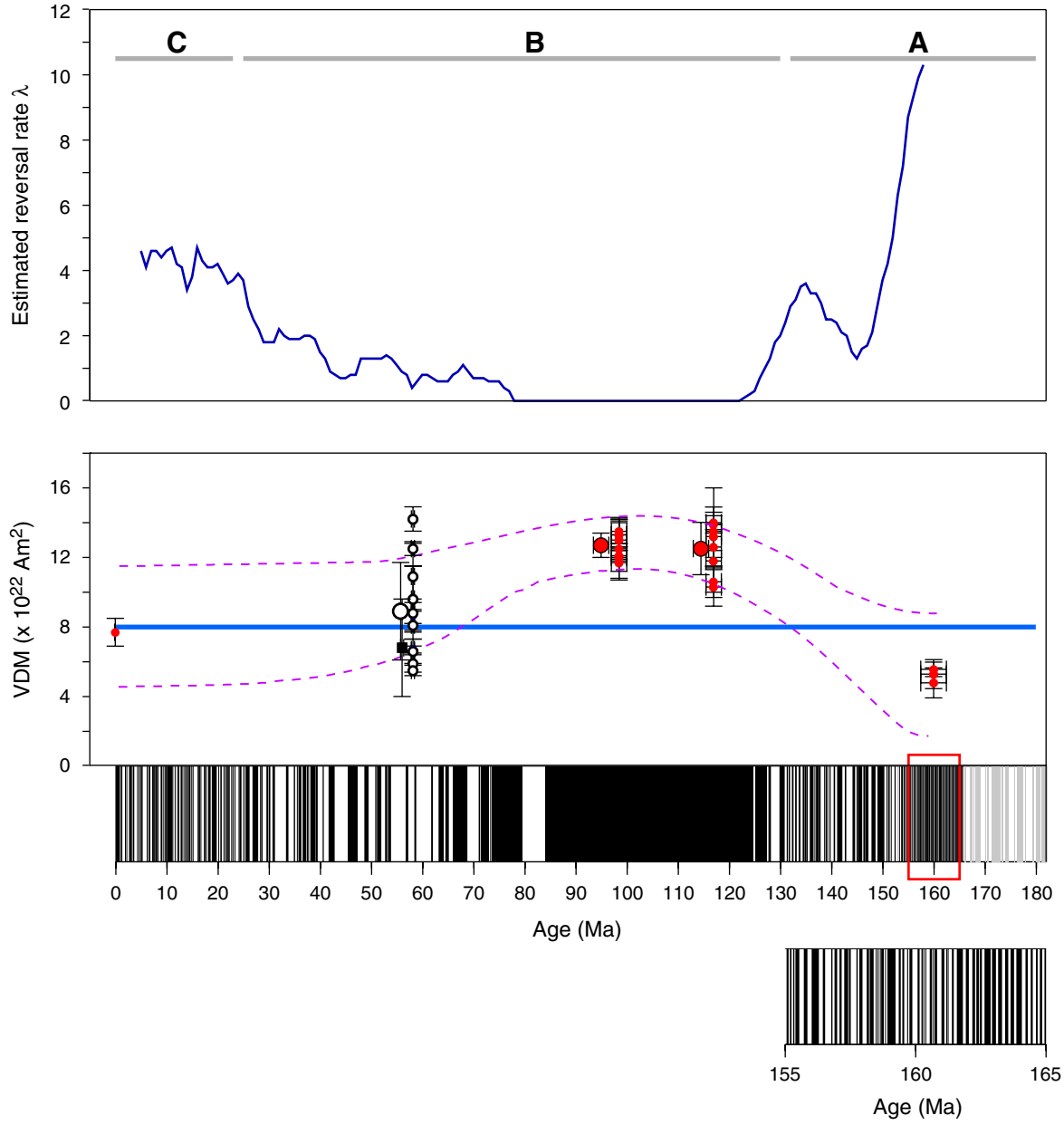

Figure F9. Age distribution of volcanic centers along the (**A**) Hawaiian-Emperor and (**B**) Louisville volcanic lineaments. Changes in rates of migration of volcanic activity are now clear for the Hawaiian-Emperor chain, and similar changes may have occurred in the Louisville chain. Age uncertainties lie within the symbols.

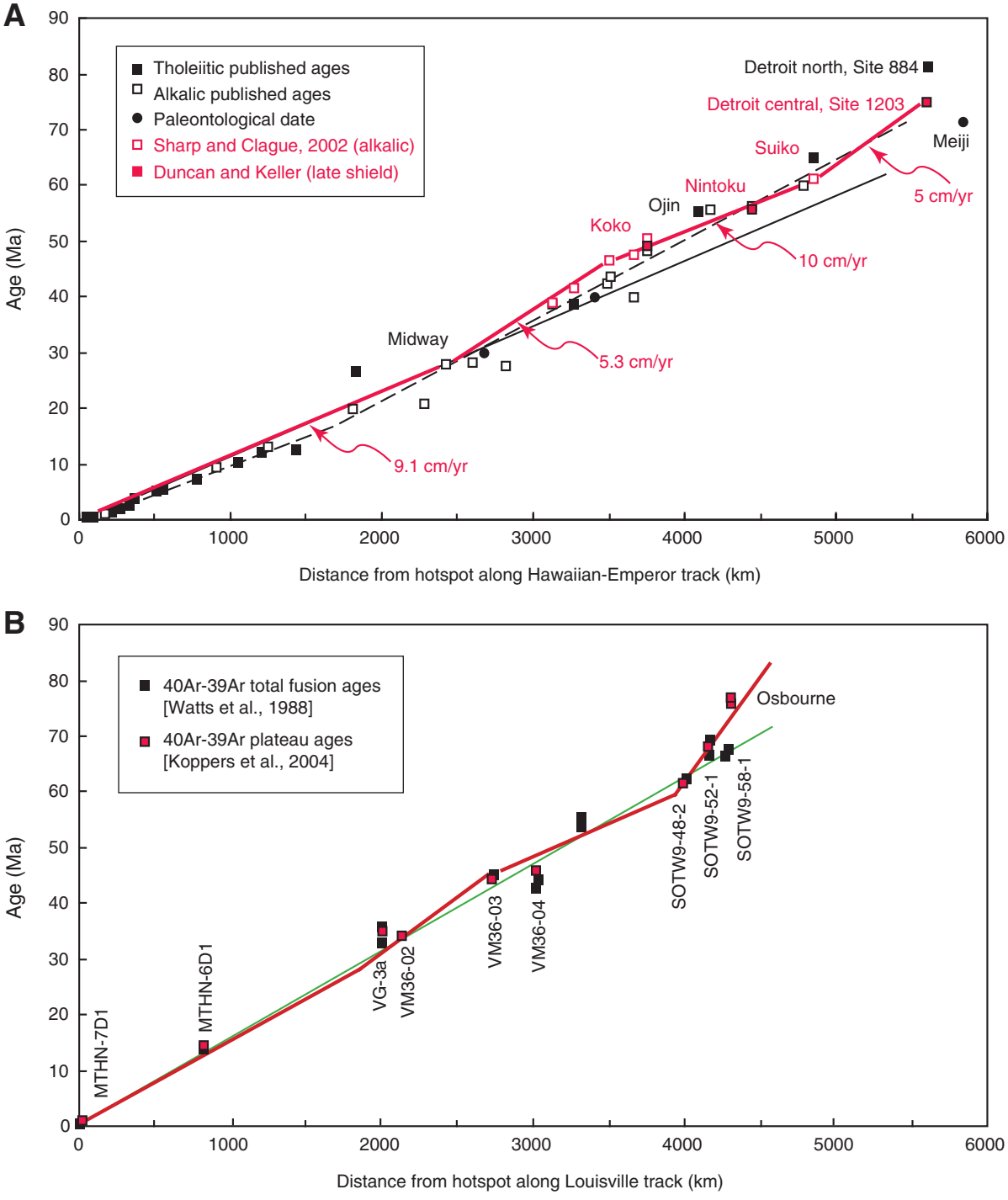

Figure F10. Computed hotspot motion and tracks for the Hawaiian and Louisville hotspots (from Koppers et al., 2004). Hotspot motion during the past 120 m.y. is shown as rainbow-colored paths, for times indicated on the colored scale bar. Tracks are shown as single-color dashed lines for Pacific fixed hotspots (black line), hotspot motion determined by Steinberger et al. (2004) (orange line), and best fit to global fixed hotspots (Steinberger et al., 2004) (gray line).

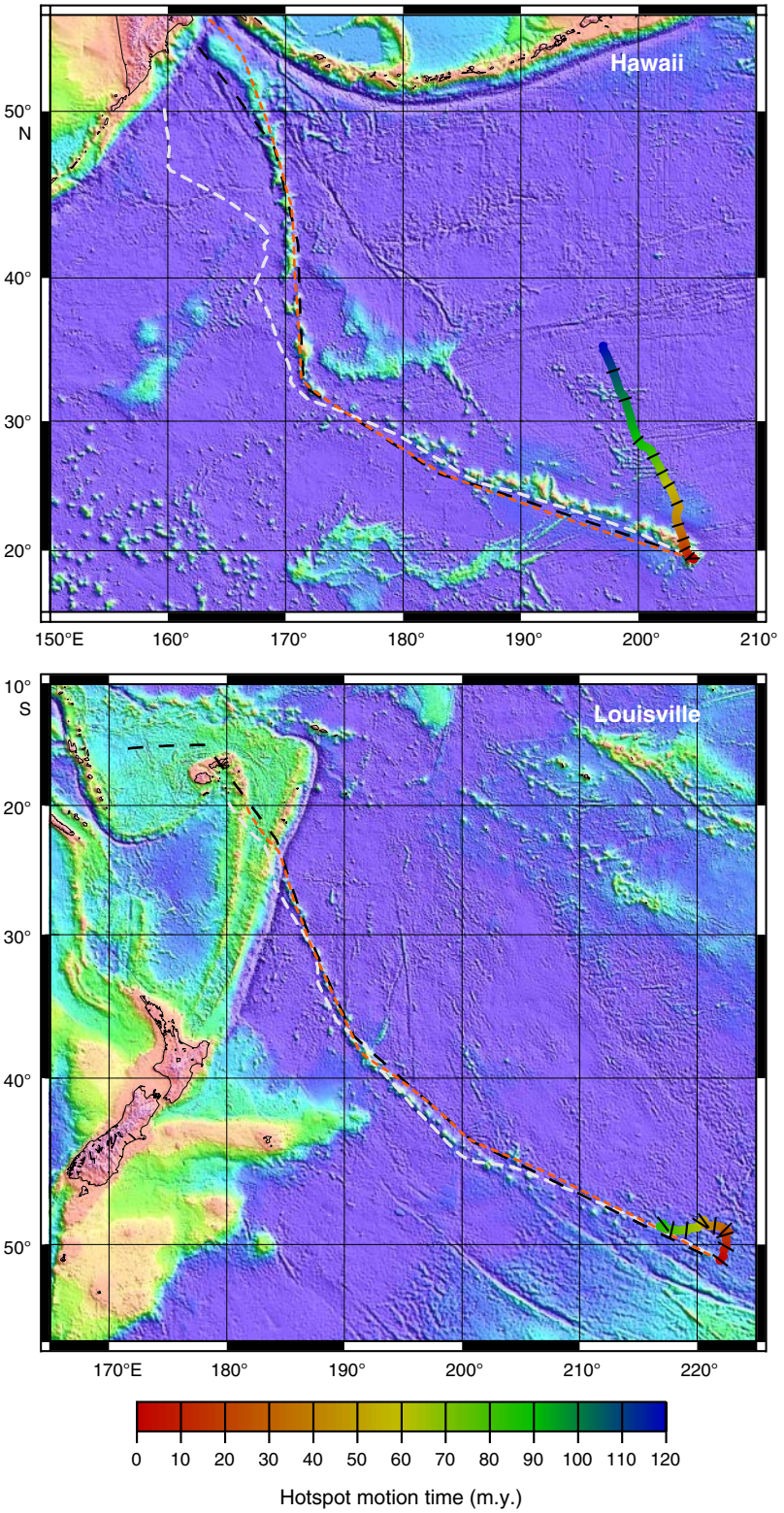

Figure F11. Models of Hawaiian volcano evolution. Preshield, main shield, postshield, and posterosional. Tectonic events may lead to volcanic eruptions much later (25–30 Ma) and postsubsidence (after Clague and Dalrymple, 1987, and references therein).

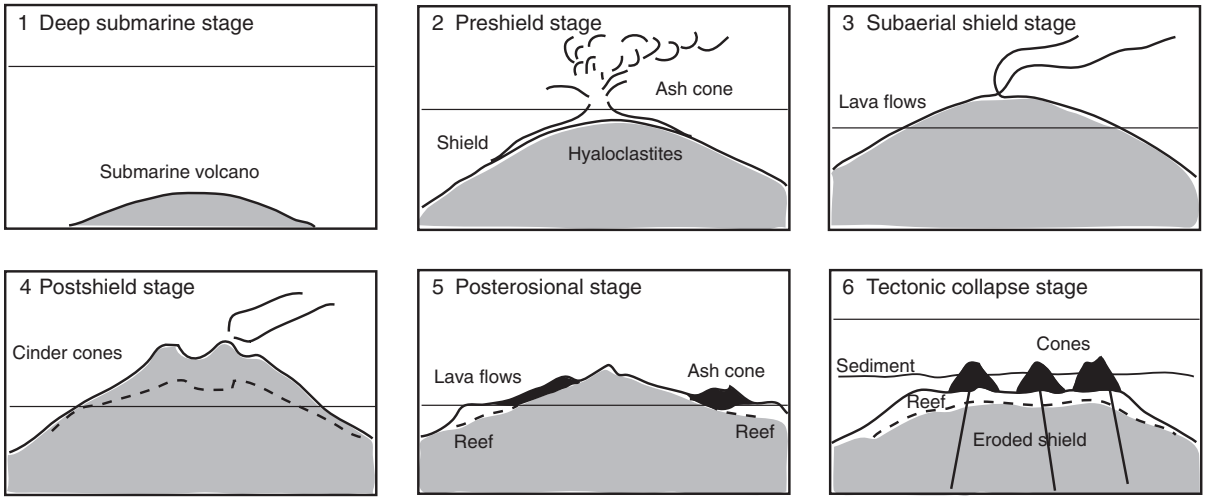

Figure F12. Volcano environment sampled by Leg 197 drilling (Tarduno, Duncan, Scholl, et al., 2002).

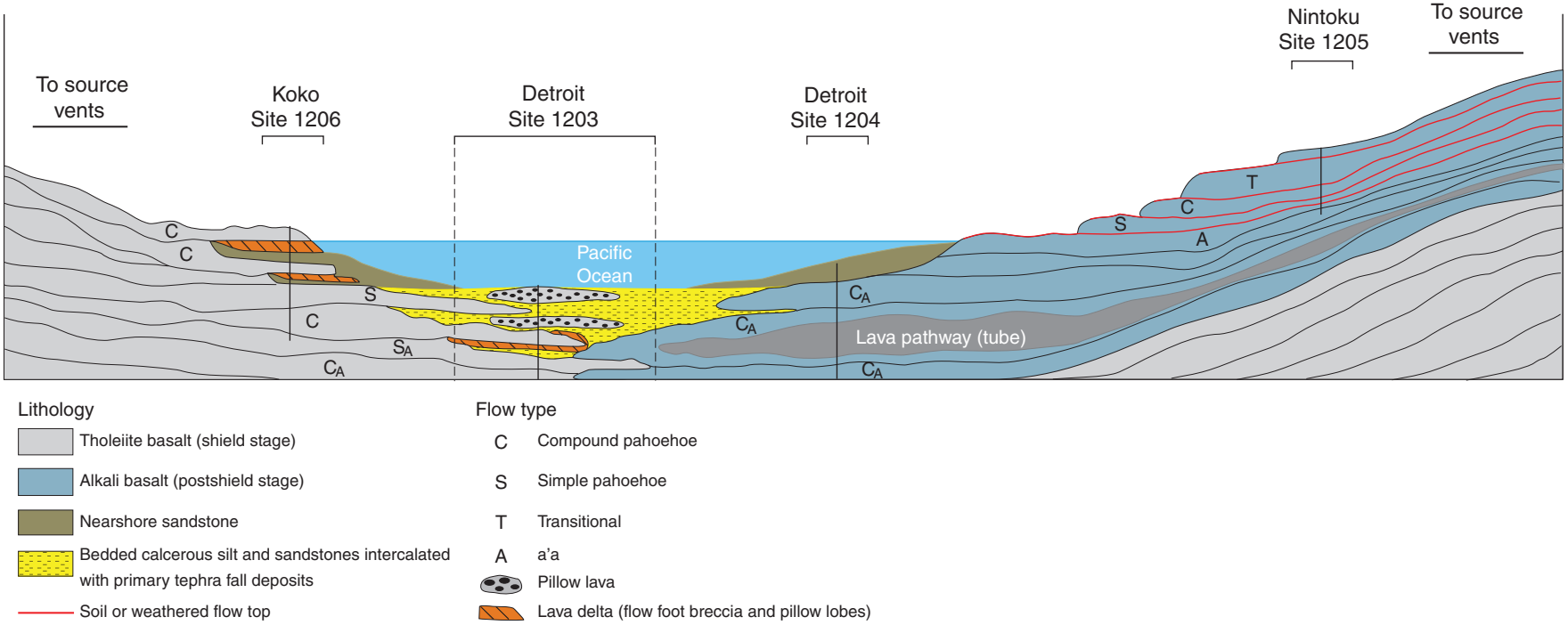

Figure F13. Major element variability ($Na_2O + K_2O$ vs. SiO_2) in the island of Hawaii, compared with Emperor Seamounts lava compositions from Leg 197 (Tarduno, Duncan, Scholl, et al., 2002).

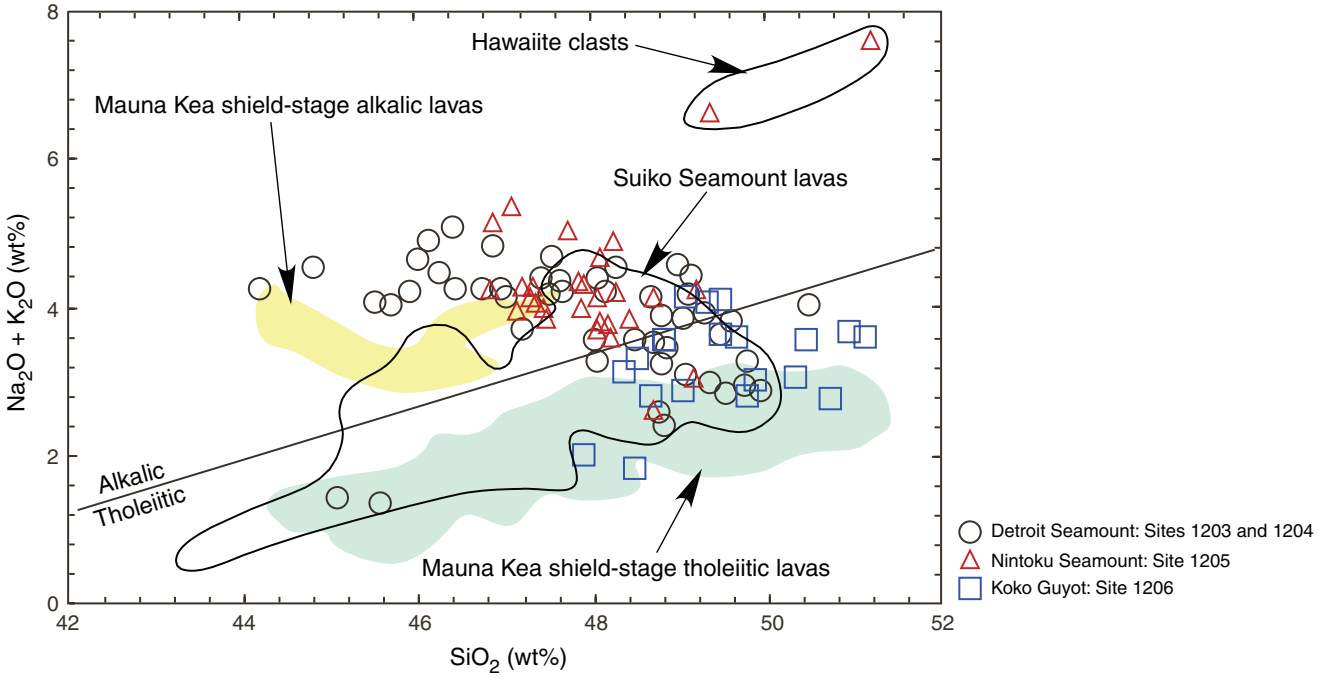

Figure F14. Sr and Pb isotopic variability at Detroit Seamount (Huang et al., 2005). Data points are for ODP Sites 883 and 884 and Sites 1203 and 1204. Detroit Seamount lavas are distinguishable from both Hawaiian Islands shield lavas and current East Pacific Ridge MORB compositions but are similar to posterosional lavas and lavas erupted on the flexural arch north of Oahu.

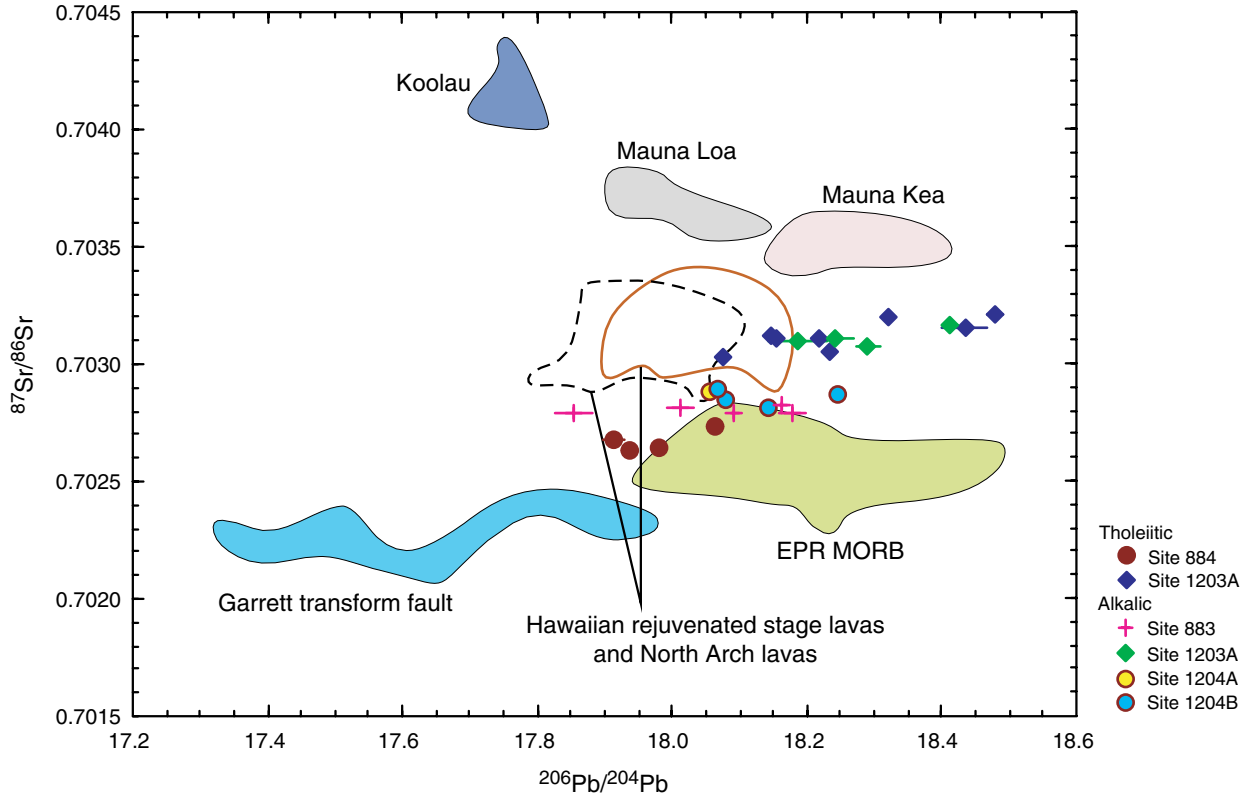

Figure F15. Isotopic variability along the Hawaiian-Emperor volcanic lineament (after Keller et al., 2004, and Frey et al., 2005). Hf isotopic compositions indicate a persistent depleted component intrinsic to the plume. He isotopic data are uniformly elevated relative to MORB but decrease toward MORB values from Suiko to Detroit Seamounts. Sr isotopic values show a progressive increase southward through the Emperor Seamounts, which is interpreted as decreasing partial mantle melting. No correlations are apparent between isotopic and magmatic volume variations (bottom panel).